processes

MDPI

Article

Development Characteristics and Distribution Patterns of Natural Fractures in the Tight Reservoirs of the Ahe Formation in the Dibei Area of the Tarim Basin

Yangang Tang [1,2,3], Yuying Wang [4,*], Liang Zhang [1,2,3], Jun Jiang [1,2,3], Hong Pang [5,*], Lin Shen [1,2,3], Guowei Zhang [1,2,3], Tiantian Zhao [1,2,3], Ling Li [1,2,3], Chang Zhou [1,2,3], Jianzhong Deng [1,2,3], Sha Li [5] and Dongxia Chen [5]

[1] Research Institute of Exploration and Development, Tarim Oilfield Company, China National Petroleum Corporation, Korla 841000, China; tangyg@petrochina.com.cn (Y.T.); zhliang-tlm@petrochina.com.cn (L.Z.); jjun-tlm@petrochina.com.cn (J.J.); shenlin-tlm@petrochina.com.cn (L.S.); zhanggw-tlm@petrochina.com.cn (G.Z.); zhaott-tlm@petrochina.com.cn (T.Z.); liling1-tlm@petrochina.com.cn (L.L.); zhouch-tlm@petrochina.com.cn (C.Z.); dengjz-tlm@petrochina.com.cn (J.D.)
[2] Research and Development Center for Ultra-Deep and Complex Reservoir Exploration and Development Technology, China National Petroleum Corporation, Korla 841000, China
[3] Engineering Research Center for Ultra-Deep and Complex Reservoir Exploration and Development, Korla 841000, China
[4] College of Science, China University of Petroleum, Beijing 102249, China
[5] College of Geosciences, China University of Petroleum, Beijing 102249, China; lisa202506@163.com (S.L.); lindachen@cup.edu.cn (D.C.)
* Correspondence: wyy1106win@163.com (Y.W.); panghong19820107@126.com (H.P.); Tel.: +86-178-6542-5226 (Y.W.); +86-152-0141-8097 (H.P.)

Abstract

In the context of the evolving global energy landscape, tight gas fields have gained increasing significance due to their low-porosity and low-permeability reservoirs, where natural fractures play a critical role in improving permeability and enhancing storage capacity. Foreland basins, such as the Dibei area in the northern Kuqa Depression of the Tarim Basin, are typical hosts for tight gas reservoirs, but the complex fracture development induced by multiple tectonic movements restricts natural gas exploration. This study employs core observation, imaging logging analysis, and thin-section microscopy to characterize the genetic types and development features of natural fractures in the Ahe Formation. Results show that 54% of natural fractures in the Dibei area are structurally originated, predominantly high-angle and open. The highest fracture density (0.351 fractures/m), six times that of other regions, occurs in the upper horst zones. Three fracture patterns are identified, namely fault–fold, fault-related, and monocline types. Fault–fold fractures are most developed due to folding and thrusting, while monocline zones are poorly fractured. Structural fractures are best developed in horst crests with fault–fold patterns. Fracture development is jointly controlled by folds, faults, stress, and lithology, with distinct characteristics across different structural positions and lithological combinations. Clarifying the development characteristics and distribution patterns of natural fractures in the Ahe Formation of the Dibei area facilitates accurate evaluation of high-quality reservoirs, providing crucial geological basis for optimizing hydrocarbon sweet spots and refining accumulation models in the region.

Keywords: Dibei area; Ahe Formation; natural fractures; development characteristics; distribution patterns

check for updates

Academic Editor: Albert Ratner

Received: 23 June 2025
Revised: 28 July 2025
Accepted: 29 July 2025
Published: 18 August 2025

Citation: Tang, Y.; Wang, Y.; Zhang, L.; Jiang, J.; Pang, H.; Shen, L.; Zhang, G.; Zhao, T.; Li, L.; Zhou, C.; et al. Development Characteristics and Distribution Patterns of Natural Fractures in the Tight Reservoirs of the Ahe Formation in the Dibei Area of the Tarim Basin. *Processes* **2025**, *13*, 2613. https://doi.org/10.3390/pr13082613

Copyright: © 2025 by the authors. Licensee MDPI, Basel, Switzerland. This article is an open access article distributed under the terms and conditions of the Creative Commons Attribution (CC BY) license (https://creativecommons.org/licenses/by/4.0/).

1. Introduction

In the global energy landscape, tight gas fields are playing an increasingly crucial role. To date, numerous tight gas reservoirs have been discovered worldwide, with the most concentrated areas being in the Rocky Mountain Basin, Arkoma Basin, Appalachian Basin, Denver Basin, San Juan Basin, and Greater Green River Basin in North America. Among them, the well-known ones include three large gas fields in the Alberta Basin of Canada, namely Elmworth, Milk River, and Hoadley, as well as twelve gas fields in the United States, such as San Juan, Uinta, Piceance, Denver, Greater Green River, Powder River, Wind River, and Raton [1,2]. For tight gas fields, the reservoir porosity and permeability are extremely low, and fluid flow mainly relies on natural fractures. The presence of natural fractures, on the one hand, significantly improves the originally poor permeability of tight reservoirs, enhances the fluidity of oil and gas, and can remarkably increase the oil and gas recovery efficiency. On the other hand, it increases the effective pore space of the reservoir, expands the oil and gas storage capacity, and creates favorable conditions for oil and gas enrichment [3]. Therefore, studying the distribution laws and development models of natural fractures in tight sandstone reservoirs is of great significance for understanding the mechanisms of oil and gas migration and accumulation. It also provides a theoretical basis for the effective development of unconventional oil and gas resources.

Globally, the dominant basin type for tight gas is the foreland basin, accounting for approximately 59%. A small portion consists of intermontane cratonic basins and continental rift basins, while a negligible fraction is made up of passive continental basins [4]. As a widespread type of tight gas basin, the foreland basin features complex geological structures. It has experienced multiple tectonic movements, resulting in intense stratigraphic deformation [5]. In recent years, significant achievements have been made in the exploration and development of tight gas in China, basically forming two major tight gas exploration domains, namely the Sulige Gas Field in the Ordos Basin and the Xujiahe Gas Field in the central Sichuan Basin of the Sichuan Basin. Tight gas reserves and production have grown rapidly, making it the most important domain for increasing natural gas reserves and production in China [6].

The Kuqa Depression is a foreland basin developed on a Paleozoic folded basement, which has mainly experienced three evolutionary stages, namely the Late Permian–Triassic foreland basin, Jurassic–Paleogene extensional depression basin, and Neogene–Quaternary regenerated foreland basin [6]. Rich in oil and gas resources, the Kuqa Depression had proven geological reserves of 1.89×10^{12} m^3 for natural gas and 1.29×10^8 t for oil by the end of 2021, with proven rates of 21.2% and 22.4%, respectively, providing a solid resource base for China's "West-to-East Gas Pipeline" project [7]. The Northern Structural Belt is located on the northern margin of the Kuqa Depression, adjacent to the Southern Tianshan Orogenic Belt. This area has superior petroleum geological conditions and huge exploration potential. Results show that the Northern Structural Belt has natural gas resources of 2.59×10^{12} m^3 and oil resources of 1.28×10^8 t, among which the proven geological reserves of tight sandstone gas and tight oil are 223×10^8 m^3 and 476×10^4 t, respectively. Its main reservoir is the Lower Jurassic Ahe Formation in the Dibei area [8].

The Dibei area has undergone multiple complex tectonic movements, such as the Late Hercynian tectonic uplift, Yanshanian compressional thrusting, and Himalayan intense thrusting. These events have rendered the development of natural fractures in the tight reservoirs of the Ahe Formation highly complex, posing numerous challenges to oil and gas exploration and development [9,10]. Under the compressional tectonic background, the characteristics and formation mechanisms of tight sandstone reservoirs remain unclear, which hinders the smooth exploration and efficient development of natural gas [11].

Previous studies have been conducted on the development of reservoirs and natural fractures in the Dibei area from multiple dimensions [12,13]. In the field of regional geological structure, it has been determined that this area is located at the front edge of the piedmont thrust fault zone on the southern slope of the Tianshan Mountains. It has experienced multiple stages of tectonic evolution, and the strata are relatively complete. Experimental studies have been carried out on the fracture development stages in the study area, and it has been concluded that the tectonic fractures can be divided into three stages, which were formed under the tectonic compression during the early, middle, and late Himalayan periods respectively. The third-stage tectonic fractures are the effective fracture-forming stage, and the controlling effect of fractures on the accumulation and transformation of tight sandstone gas reservoirs has been clarified [14]. However, the development characteristics of natural fractures in the Dibei area remain unclear, and systematic research on their distribution patterns is lacking. Previous studies have classified fractures in this area into tectonically and sedimentologically originated types [15], yet the criteria for such classification and their specific distribution in the region remain undefined. Some scholars have indicated that fractures are most developed in high tectonic positions on the plane [16], but research into the detailed characteristics of fracture development under different microstructural units remains inadequate. Additionally, while some studies have noted that lithology influences fracture development, with coarser sandstones exhibiting more fractures [17], research on the variations in fracture development across different sedimentary cycles and the impact of lithological associations on the vertical distribution of fractures remains relatively superficial. In the analysis of main controlling factors, although such factors as folds, faults, stress, lithology, and sand-body thickness have been proposed [18], the coupling relationships among these factors and their dynamic influence mechanisms on fracture development in different geological historical periods have not been systematically and thoroughly explored.

Against this background, to clarify the genetic types of natural fractures in the tight sandstone reservoirs of the Ahe Formation in the Dibei area, identify their developmental characteristics and distribution patterns in planar and vertical directions, and to reveal the controlling factors of natural fractures in this area, this study employs multiple technical methods, such as core observation, imaging logging analysis, and microscopic thin-section analysis. It conducts an analysis of the planar distribution, genetic characteristics, and differences in fractures. A thorough investigation is carried out on the genetic types and distribution characteristics of natural fractures in this area. By integrating the tectonic styles of the region, a distribution pattern of natural fractures in the Ahe Formation of the Dibei area is established. Through a combination of tectonic, reservoir, and stress analyses, the controlling factors and influence mechanisms of natural fractures are elucidated. In existing studies of this area, the distribution characteristics and main controlling factors of fractures remain unclear, with a lack of research on natural fracture development models [19]. This study fills the theoretical gap, provides support for determining favorable reservoirs and predicting favorable accumulation zones in the Dibei area, and holds significant practical significance for guiding oil and gas exploration and development in this region.

2. Materials and Methods

2.1. Regional Geological Overview

The Tarim Basin is the largest oil-and-gas-bearing basin in China. Its intricate tectonic evolution history has significantly influenced the geological features of diverse regions within the basin. The Dibei area is situated in the northern part of the Kuqa Depression in the Tarim Basin, at the front of the piedmont thrust fault zone on the southern slope of the Tianshan Mountains (Figure 1). It is approximately 88 km southwest of Kuqa City, Aksu

Prefecture, Xinjiang [20]. This area holds a vital position in the regional geological structure framework, and its geological characteristics play a crucial role in in-depth research on the generation, migration, and accumulation of oil and gas in the basin.

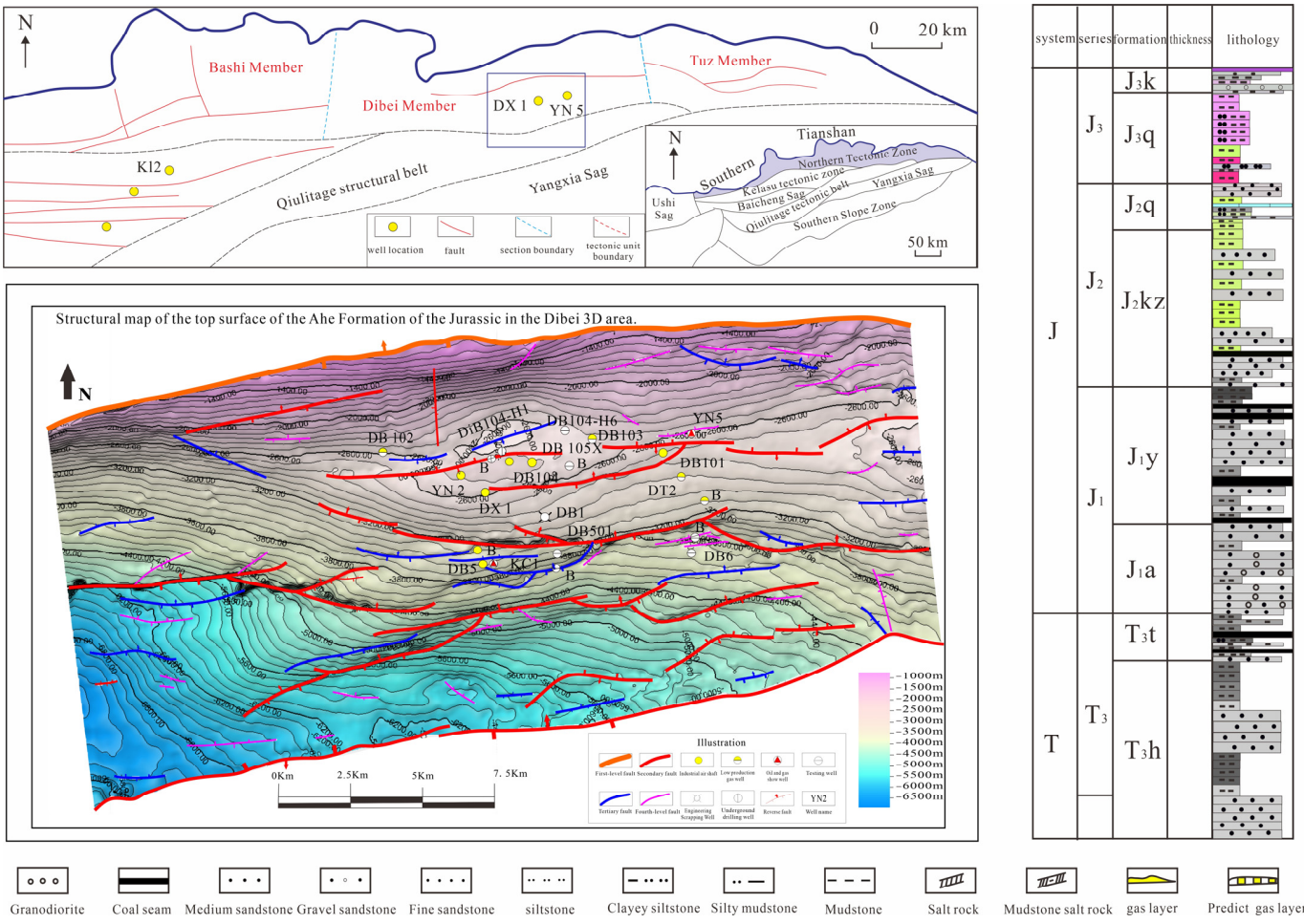


Figure 1. The tectonic location of the Dibei area and the top surface structure of the Ahe Formation.

In terms of stratigraphic development, the strata exposed in the Dibei area are relatively complete. They successively include the Cambrian, Ordovician, Silurian, Devonian, Carboniferous, and Permian of the Paleozoic, the Triassic, Jurassic, and Cretaceous of the Mesozoic, as well as the Paleogene, Neogene, and Quaternary of the Cenozoic [21]. Among them, the Ahe Formation, an essential reservoir interval in the study area, is mainly developed at the base of the Jurassic. It is a sandstone formation primarily deposited by braided rivers. The sandstone of the Ahe Formation is extensively distributed across the region, with a wide range of thicknesses, typically from tens of meters to over a hundred meters. Its lithology mainly consists of medium-to-coarse-grained sandstone and gravel-bearing sandstone, featuring relatively low compositional and structural maturity. The quartz content generally ranges from 50% to 70%, while the feldspar and lithic fragment contents are relatively high [22]. This provides a certain material basis for the subsequent development of natural fractures.

In terms of tectonic evolution, the Dibei area has experienced multiple tectonic movements. During the Early Paleozoic, the Tarim Plate was in a relatively stable craton development stage, and the Dibei area mainly received stable marine sedimentation. Since the Late Paleozoic, influenced by the collision and amalgamation of surrounding plates, the Tarim Basin entered a period of intense tectonic deformation [23]. Especially during the

Mesozoic, under the influence of the Indosinian and Yanshanian movements, the internal tectonic pattern of the basin changed significantly. The Dibei area began to be affected by compressive stress, forming a series of NE–SW trending folds and fault structures [24]. These tectonic movements not only altered the original occurrence of the strata but also generated a large amount of tectonic stress within the rocks, creating favorable conditions for the formation of natural fractures [25,26]. In the Cenozoic, strongly influenced by the Himalayan movement, the piedmont thrust fault zone on the southern slope of the Tianshan Mountains further uplifted. The tectonic deformation in the Dibei area became more complex, causing the pre-existing fractures to expand and transform, and also generating some new fracture systems [27].

In summary, the Dibei area in the Tarim Basin has experienced multiple tectonic movements. The Ahe Formation, an important reservoir interval in the study area, is located at the bottom of the Jurassic. Under the combined action of multiple factors, such as the regional geological background, stratigraphic development, tectonic evolution, and rock mechanical properties, the current complex geological features have been formed. These features play a crucial controlling role in the development of natural fractures in the tight reservoirs of the Ahe Formation and provide an important geological basis for in-depth research on the characteristics of oil and gas reservoirs and exploration and development in this area.

2.2. Samples and Data

We retrieved core samples from 10 cored wells in the Kuqa Depression. To better document lithology, sedimentary structures, and natural fractures, we collected 360° scanned core surface photographs. A total of 869 core samples were observed and recorded; detailed records and descriptions of natural fractures and lithology of the cores were then made. Thin sections (30-micrometers-thick) impregnated with blue- or red-dyed resin were utilized to detect pore spaces. Additionally, imaging logging data from 8 wells were collected, and a total of 549 fractures of various types were identified and screened. In addition, we have also collected structural data, such as in situ stress data and fault activity intensity data in the area, to draw relevant maps. The detailed process is shown in Figure 2.

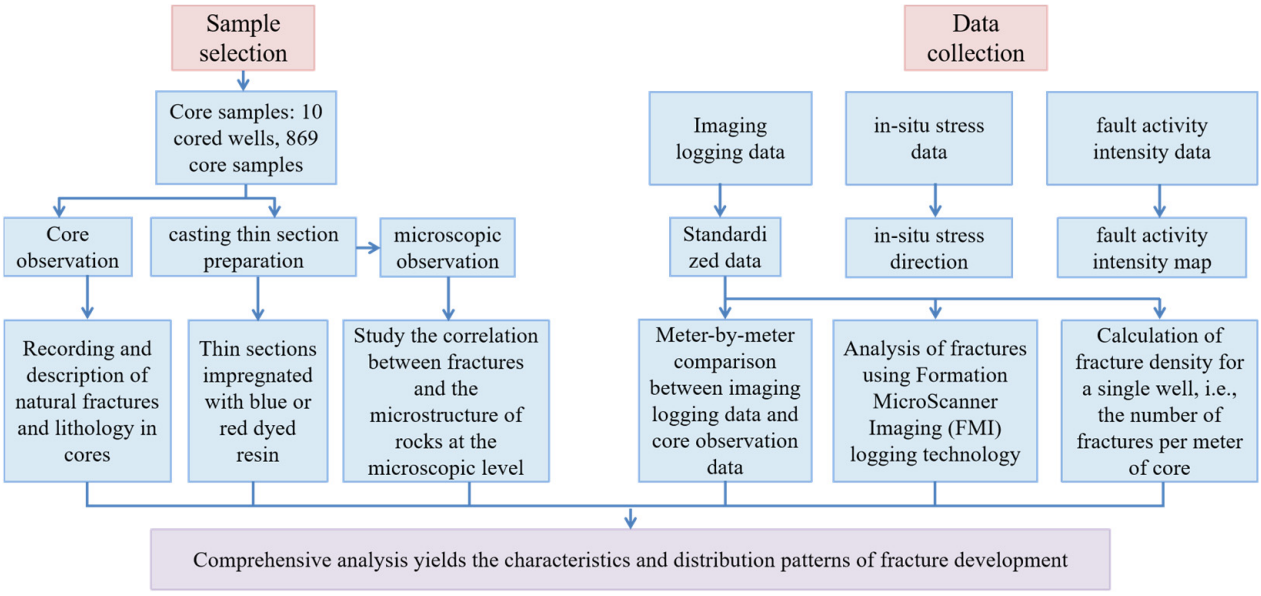


Figure 2. Flow chart of the research methodology.

Preparation of rock cast thin sections: Core samples from the Jurassic Ahe Formation in the Dibei area were selected, and cylindrical samples of 2.5 cm × 5 cm were cut. Impurities were removed using an SYD-2000 core cleaning instrument (manufactured by Haian Core Petroleum Instrument Co., Ltd., Haian, Jiangsu, China; power 500 W, pressure 0.3 MPa, 500 W, 0.3 MPa). The samples were then dried to constant weight in a DHG-9070A constant temperature drying oven (manufactured by Shanghai Fuxu Laboratory Instrument Equipment Factory, Shanghai, China; ±1 °C precision) at 60 °C for 48 h. E-44 epoxy resin (produced by Sinopec Baling Petrochemical Co., Ltd., Yueyang, Hunan, China) and ethylenediamine curing agent (manufactured by Muby Chemicals of Muby Chem Group, Ambernath, Mumbai, India) were mixed at a 5:1 ratio and stirred for 10 min using a JJ-1 stirrer (300 r/min; manufactured by Changzhou Langyue Instrument Manufacturing Co., Ltd., Changzhou, Jiangsu, China). The cores were placed in a ZK-3 vacuum impregnation (manufactured by German Heinrich Vacuum Equipment Co., Ltd., Xiamen, Fujian, China; pressure ≤0.098 MPa), evacuated for 30 min, then injected with the casting agent and held under pressure for 24 h. Subsequent curing was performed in an HH-S constant temperature water bath at 60 °C for 48 h. Sections of 0.5 mm thickness were cut using a Q-2 slicer (diamond blade, rotational speed 2800 r/min; manufactured by Shanghai Yanrun Optical Machine Technology Co., Ltd., Shanghai, China), then progressively ground to 30 μm using XQ-1 metallographic sandpaper (400 → 1200 grit, manufactured by Shanghai Yanrun Optical Machine Technology Co., Ltd., Shanghai, China). Flatness was controlled with an MP-2B grinder (manufactured by Jinan Kason Testing Equipment Co., Ltd., Jinan, Shandong, China), and thickness error (≤2 μm) was verified using a reading microscope (0.01 mm precision, manufactured by British Industrial Microscope Co., Ltd., Warwickshire, UK).

2.3. Theory and Methodology

This study comprehensively applies multiple theories and methods to deeply analyze the development characteristics and distribution patterns of natural fractures in the tight reservoirs of the Ahe Formation in the Dibei area.

To obtain standardized fracture data for the 10 wells in the study area, fracture densities extracted from imaging logs were compared meter-by-meter with those measured from cores, with the consistency rate calculated (requiring ≥80%). For intervals with deviations exceeding 20% (e.g., missed or over-identified fractures in imaging logs), corrections were made by readjusting the identification thresholds. Automatically identified fracture data were reviewed by at least two interpreters. For fractures with significant discrepancies, such as differentiation between induced and natural fractures, determinations were made by observing the presence of infillings in core thin sections under a microscope. To scientifically compare fracture development across different wells, fracture parameters were standardized: the fracture density of each well was calculated with a unified unit of fractures per meter (i.e., the number of fractures per meter of core), eliminating differences caused by varying sampling lengths.

Core observation is a crucial fundamental method. Based on the theories of petrology and structural geology, the cores are carefully observed [28]. The occurrence of natural fractures (strike, dip, and dip angle) is accurately recorded, which can visually represent the spatial distribution of fractures. The morphological characteristics of fractures, such as straightness, curvature, and branching, are described. These characteristics are closely related to the origin of fractures. Attention is also paid to the characteristics of fracture fillings. For example, calcite-filled fractures may imply late-stage hydrothermal activities, which helps to preliminarily determine the genetic types of fractures [29].

Imaging logging analysis is based on the principles of geophysics and utilizes the Formation MicroScanner Imager (FMI) technology [30]. This technology generates high-resolution images by measuring the resistivity changes in the formation on the wellbore wall, enabling clear identification of fractures. Subsequently, the fracture width, a key parameter for evaluating fracture effectiveness, as wider fractures have better seepage capabilities, is accurately measured, and the fracture density, which is closely related to oil and gas storage and migration, is statistically analyzed. By processing and analyzing the imaging logging data, the strike and dip angle of fractures can be determined. This verifies the results of core observation and improves data accuracy [31]. Moreover, imaging logging can obtain a wide range of fracture information, compensating for the limitations of core observation and enabling macroscopic control over the planar and vertical distribution characteristics of fractures.

A Leica DM4P polarizing microscope, equipped with a 5-megapixel DFC450C camera (manufactured by Leica Microsystems, Wetzlar, Germany) and supporting plane-polarized light, cross-polarized light, and fluorescence modes (magnification 50×–400×, resolution 0.5 μm), was used. 30 μm-thick thin sections were placed under the microscope to examine the correlation between fractures and the rock microstructure at the microscopic scale [32]. The interaction between fractures and mineral grains, such as whether fractures follow grain boundaries or cut through grains, is analyzed to understand the influence of rock mechanical properties on fracture formation. The modification of the rock pore structure by fractures is studied, with attention paid to the connectivity between fractures and pores and the impact on pore development or destruction, which, in turn, affects the porosity and permeability of the reservoir. This helps to determine the micro-origin of fractures and provides microscopic evidence for fracture origin research [33].

3. Results

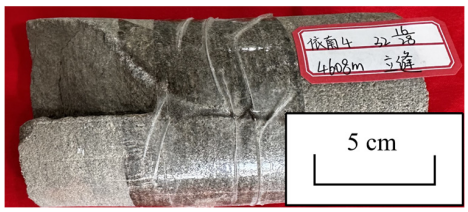
3.1. Development and Distribution Characteristics of Natural Fractures

3.1.1. Fracture Origins and Classification

The genetic types of natural fractures include tectonic fractures, diagenetic fractures, fractures formed by volcanic activity, hydraulically induced fractures, and gravity induced fractures [34]. Results from core and thin section observations as well as imaging logging interpretation show that natural fractures are relatively well developed in the tight reservoirs of the Ahe Formation in the Dibei area of the Tarim Basin. Among them, the thickness of rock layers in the fracture developed sections accounts for approximately 53.2% of the total thickness of the core observation sections. The natural fracture types in the Ahe Formation reservoirs of the study area are mainly tectonic fractures and diagenetic fractures, with tectonic origin fractures being dominant.

The formation of diagenetic fractures is related to such factors as rock volume forces, gravity, or diagenetic processes [35]. During the diagenesis of rocks, stress changes occur within the rock due to compaction, cementation, dissolution, and other processes. When these stresses exceed the strength of the rock, diagenetic fractures are formed [36]. For example, during compaction, the rearrangement of rock grains reduces porosity, which may lead to the formation of micro-fractures within the rock. Additionally, the uneven distribution or dissolution of cement can also trigger the formation of diagenetic fractures [37]. Morphologically, sedimentary-origin fractures mainly present as flat fractures, bedding fractures, and low-angle fractures [38] (Table 1). Flat fractures have a fracture angle of 0–10° and develop along the bedding of the strata. Low-angle fractures, with angles between 10–30°, are also closely related to sedimentary bedding. In core observations, distinct bedding-fracture features can be seen, and bedding fractures extend along the bedding plane, reflecting the control of the sedimentary environment on fracture formation.

Table 1. Core photos of natural fractures in the Ahe Formation of the Dibei area.

Fracture Type	Fracture Dip Angle	Core Photos
Sedimentary origin fractures	0–10°	 Well YiNan 5 (YN 5), 4842.23 m
	10–30°	 Well DiBei 105X (DB105X), 4768.85 m
Tectonic origin fractures	30–60°	 Well DiTan 2 (DT 2), 5098.50 m
	60–80°	 Well DiBei 102 (DB102), 5053.50 m
	80–90°	 Well YiNan 4 (YN 4), 4608.00 m

The formation and development of tectonic fractures are controlled by factors, such as lithology and tectonics. Under the action of tectonic stress, rocks rupture to form tectonic fractures [39]. The complexity and multi-episodic nature of tectonic movements endow tectonic fractures with diverse morphologies and occurrences. The Dibei area, located in the northern part of the Kuqa Depression, has been influenced by multiple tectonic movements, including the Indosinian Movement, Yanshanian Movement, and Himalayan Movement. The compressional and tensional stresses generated by these movements serve as the primary driving forces for the formation of tectonic fractures [40]. In terms of rock mechanical properties, rocks with higher brittleness, such as the quartz-rich medium-to-coarse-grained sandstones in the Ahe Formation, are more prone to rupture and form tectonic fractures under tectonic stress [41].

Morphologically, due to the effect of tectonic stress, these fractures are characterized by large angles and strong extensibility [42], and they are the main type of fractures in the study area. They can be further divided into inclined fractures with angles ranging

from 30° to 60°, which may be formed by the tectonic transformation of bedding fractures or direct tectonic actions; high-angle fractures with angles from 60° to 80°, which are the products of concentrated release of tectonic stress; and vertical fractures with angles 80–90°, which are nearly perpendicular to the strata. Core observations show that at certain depths, such as 5053.5 m in Well DB102 and 4409.5 m in Well YN 4, high-angle and vertical fractures cut through the rocks, indicating the strong influence of tectonic movements. Imaging logging shows that the density of high-angle fractures in the entire section of Well DB104 is relatively large in the vertical direction (Figure 3a). This is probably because Well DB104 is located in a high-structural position, where it is prone to forming high-angle tectonic fractures due to the influence of compressive stress and paleo-structures.

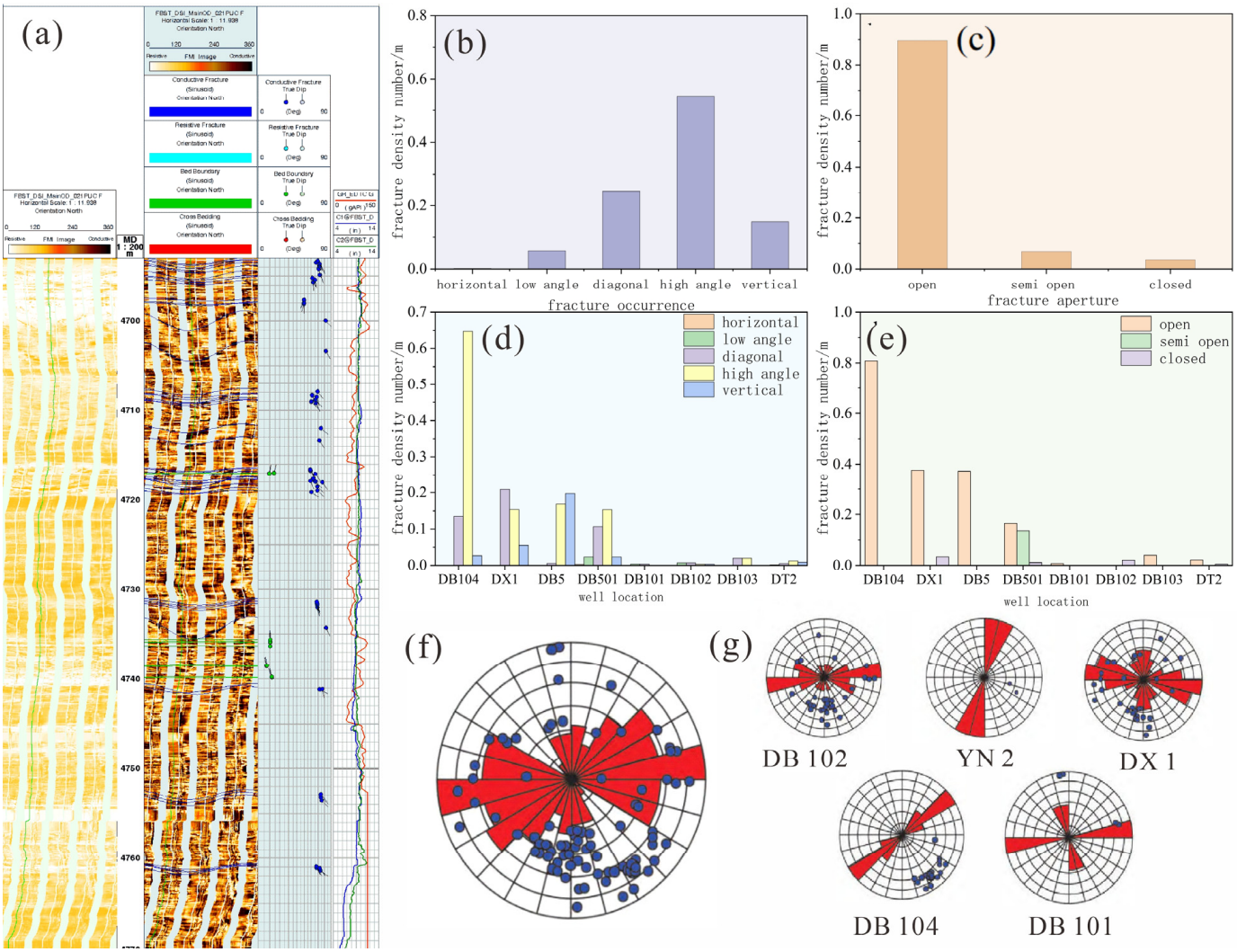


Figure 3. (**a**) Imaging logging image of Well DB104 at a depth of 4765–4770 m; (**b**) Statistical chart of fracture occurrences in the Dibei area; (**c**) Statistical chart of fracture apertures in the Dibei area; (**d**) Statistical chart of fracture occurrences at different well locations; (**e**) Statistical chart of fracture apertures at different well locations; (**f**) Statistics of the overall fracture strike (red) and dip (blue) in the Dibei area; (**g**) Statistics of the fracture strike (red) and dip (blue) of a single well [43].

3.1.2. Fracture Distribution Characteristics

(1) Fracture Occurrences and Development Degrees

The fractures in the study area are mainly high-angle fractures and open fractures; among them, high-angle fractures account for approximately 54.6%, with open fractures comprising around 89.6% (Figure 3b,c). Their planar distribution is significantly controlled

by the structural position, following the development pattern of "the high part of the fault-block zone > the southern slope > the low part of the fault-block zone" (Figure 4). The high part of the fault-block zone, as the area where tectonic stress is concentrated and released, has the highest degree of fracture development. For example (Figure 3d,e, Table 2), taking Well DB 104 as an example, the number of open fractures reaches 60, with a density of 0.809 fractures/m and a high-angle fracture density of 0.547 fractures/m. The fractures in Well DB 104 are mainly high-angle open fractures, indicating good fracture development. In Well DX1, the density of open fractures is 0.376 fractures/m, with well-developed inclined fractures and high-angle open fractures, showing a relatively good development situation. The low part of the fault block zone has weak tectonic stress and poor fracture development. For example, Well Dibei 102 exhibits poor fracture development, with a low fracture density of 0.021 fractures/m, dominated by bedding and oblique fractures, all of which are closed. In Well DB101, the entire cored interval of the Ahe Formation contains one low-angle fracture and one oblique fracture, resulting in a fracture density of 0.004 fractures/m, indicating poor development. Well DT2, located in the low part of the horst zone, has a high-angle fracture density of 0.013 fractures/m, along with a small number of low-angle and oblique fractures, predominantly open ones. The fracture development degree in the southern slope is between that of the high and low parts of the fault block zone. In Well DB5, located in the high part of the southern slope, the fracture density is 0.372 fractures/m, with developed bedding fractures, vertical fractures, and high-angle open fractures, presenting a relatively good development situation. In Well DB501, located in the relatively high part of the southern slope, there are 113 open fractures with a density of 0.16 fractures/m, and inclined fractures, high-angle open fractures, and semi-open fractures coexist, also showing a relatively good development situation.

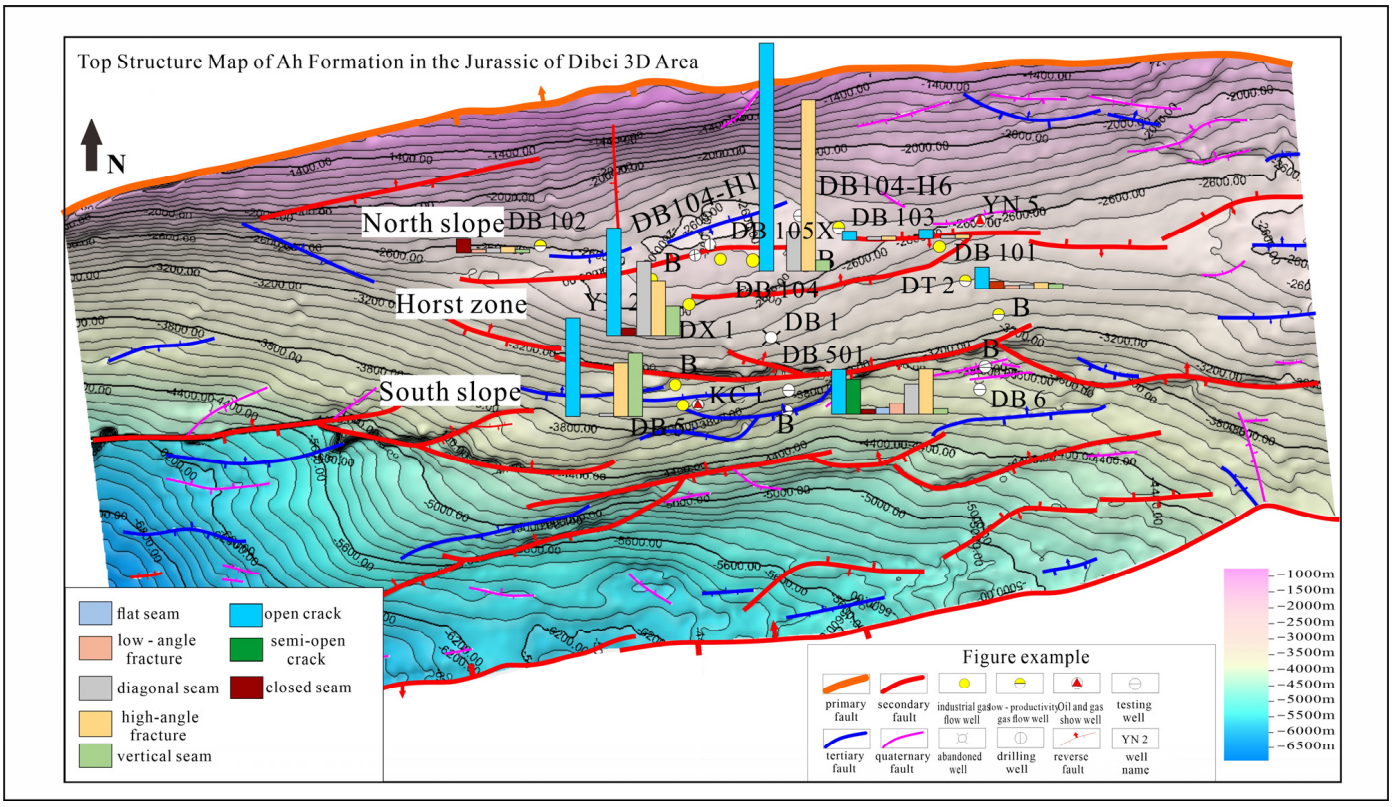


Figure 4. Planar distribution characteristics of fractures in the Ahe Formation of the Dibei area based on imaging logging.

Table 2. Distribution of the number of fractures and fracture densities in different regions (unit: strips/density strips/m).

Regional Distribution		Well Name	Fracture Filling Status			Fracture Dip Angle Types					Density	Bedding Fractures	Fracture Development Status
			Closed Fractures	Semi-Open Fractures	Open Fractures	Vertical Fractures	High-Angle Fractures	Inclined Fractures	Low-Angle Fractures	Horizontal Fractures			
Fault terrace zone area	High position of the fault terrace zone	DB 104			60/0.809	2/0.027	48/0.547	10/0.135			0.809		Good
		DX1	8/0.034		88/0.376	13/0.056	36/0.154	47/0.200			0.41		Relatively good
	Low position of the fault terrace zone	DB 101			2/0.008		1/0.004	1/0.004			0.008		Poor
		DB 102	6/0.021			1/0.003	2/0.007	3/0.011			0.021	5/0.087	Poor
		DB 103			2/0.04		1/0.02	1/0.02			0.04		Poor
		DT 2	3/0.006		12/0.022	5/0.009	6/0.012	3/0.006	1/0.001		0.029		Relatively poor
Southern slope	High position of the southern slope	DB 5			64/0.372	34/0.197	29/0.169	1/0.006			0.372	16/0.882	Relatively good
	Low position of the southern slope	DB 501	8/0.117	93/0.135	113/0.16	16/0.023	107/0.153	73/0.106	16/0.023	2/0.002	0.31	2/0.076	Relatively good

(2) Distribution Regularities of Fracture Strikes

The fracture occurrences exhibit three systems, namely nearly EW-trending, NE-trending, and nearly SN-trending. Through comprehensive analysis of imaging logging and core data, it is found that nearly EW-trending fractures are the most widely developed, followed by NE-trending fractures. The fracture strikes are mostly parallel to the trends of regional faults [43] (Figure 3f,g). Statistical analysis of imaging logging data shows that high-angle fractures account for 49.8%, being the dominant fracture type, while flat fractures and low-angle fractures are scarce, accounting for only 4.33%. Well DB 104 provides clear evidence that high-angle fractures are densely developed within the well interval, thus confirming the dominant role of high-angle fractures in the planar distribution (Figure 3a).

3.2. Natural Fracture Development Models

3.2.1. Classification of Tectonic Styles

In the study of tight reservoirs in the Ahe Formation of the Dibei area, Tarim Basin, tectonic styles play a crucial controlling role in the development of natural fractures [44]. Tectonic styles can be classified into four types, namely fault–fold–fracture type, fault–fracture type, fold–fracture type, and monocline type. Different tectonic styles exhibit distinct differences in fracture development characteristics and controlling factors [45] (Figure 5).

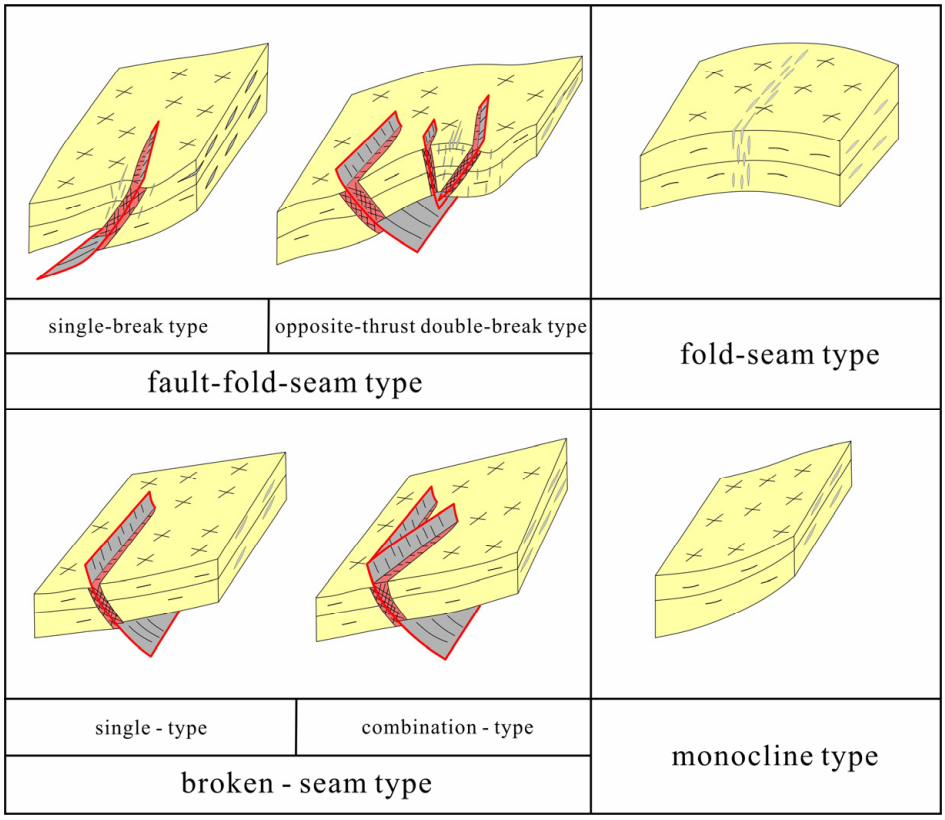


Figure 5. Division model of fault–fold–fracture structure styles in the Ahe Formation of the Dibei area.

(1) Fault–Fold–Fracture Type

In the fault–fold–fracture tectonic style, the formation of fracture zones is closely related to the folds generated during the compression process and the activity of reverse faults. Under the intense action of tectonic stress, the strata undergo folding deformation, accompanied by the activity of reverse faults. This complex tectonic environment causes numerous fractures within the rocks, thus forming a well-developed fracture zone [45]. This type of tectonic style reflects the strong compressive effect of regional tectonic stress,

providing sufficient power and deformation space for the formation of fractures. As shown for the single-break type in Figure 5, displacement occurs along a single fracture, resulting in the formation of strata folds. The development of fractures in this tectonic style is controlled by both the single fault and the strata folds. Fractures develop along the fault- and fold-related stress concentration zones, with the fault dominating tectonic deformation. In contrast, the opposite-thrust double-break type involves two opposing faults. Bidirectional compression induces more complex stratal folding with intense faulting; fractures are densely distributed between faults and in folded zones, with tectonic deformation governed by the two faults' opposing thrusting.

(2) Fault–Fracture Type

The fault–fracture tectonic style is mainly associated with the activity of reverse faults, but without significant folding. Studies show that the closer the distance to 2–3-grade faults (within 600 m), the greater the number of developed fractures, while the control effect of 4-grade faults on fracture development is relatively limited [46]. The stress concentration caused by the activity of reverse faults leads to the fracturing of rocks near the faults. This type of tectonic style emphasizes the dominant role of reverse fault activity in fracture formation and reflects the correlation between fault grade and fracture development degree. As shown for the single-fault–fracture type in Figure 5, dominated by a single fault activity, the fault cuts through strata, generating fractures in and near the fault zone due to stress release and rock fragmentation; fracture development is controlled by the single fault, with relatively simple structural styles. In contrast, the composite fault–fracture type is affected by the combined action of multiple faults, which mutually cut and influence each other, resulting in complex tectonic deformation. Fractures are extensively developed in the interaction zones of multiple faults, representing a typical type of complex fracture system formed by the synergistic effect of multiple faults.

(3) Fold–Fracture Type

Under the fold–fracture tectonic style, the fracture zone is mainly controlled by the formation and activity of paleo-uplifts. During the formation and evolution of paleo-uplifts, the surrounding strata are subjected to varying degrees of stress, resulting in rock fracturing and the formation of fractures [46]. The activity history and scale of paleo-uplifts have a significant impact on the distribution and development degree of fractures. As shown for the fold–fracture type in Figure 5, strata are dominated by folding deformation, without obvious control by large-scale faults. Interlayer sliding and stress concentration induced by folding promote fracture development along fold limbs and axes; fracture distribution is closely associated with fold geometry, representing a typical type of fold-derived fractures.

(4) Monocline Type

The monocline tectonic style occurs in areas that have not been significantly affected by tectonic activities, and no obvious fracture zone is formed. In this tectonic style, the strata are relatively stable, lacking sufficient tectonic stress to promote the formation of large-scale fractures. Therefore, the degree of fracture development is poor [47]. As shown for the monocline type in Figure 5, strata present a gently dipping monocline morphology. Sparse fractures are generated in the monocline strata due to regional tectonic stress or differential sedimentation. Tectonic deformation is dominated by simple tilting, with relatively low fracture development, which is controlled by the monocline stress field.

3.2.2. Fracture Development Models

(1) Fault–Fold–Fracture Type

In the fault–fold–fracture tectonic style, the distribution of fractures is jointly controlled by faults and folds. In such a complex tectonic environment, rocks are subjected to intense compression and deformation, resulting in the relatively well-developed inclined fractures and high-angle open fractures (Figure 6). In terms of lithology, these fractures are concentrated in thin-bedded coarse sandstone and conglomeratic coarse sandstone. This is because coarse-grained rocks are inherently more brittle. Under the stress generated by fault and fold activities, they are more likely to rupture and form fractures. Moreover, thin-bedded coarse sandstone has relatively fewer constraint conditions under tectonic stress, making it easier to generate fracture surfaces, thus promoting the formation of inclined fractures and high-angle open fractures.

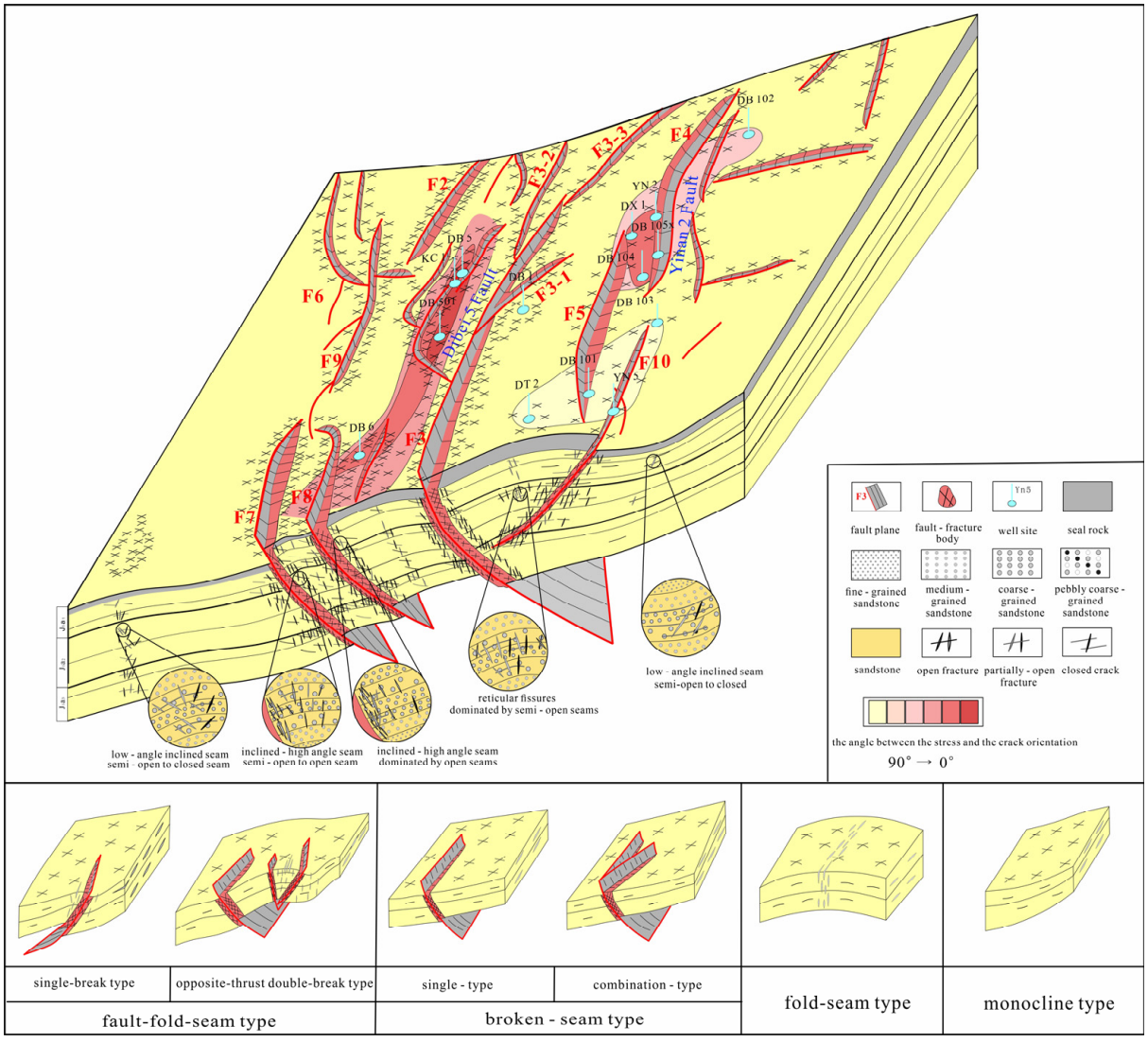


Figure 6. Development and distribution patterns of fractures in the Ahe Formation of the Dibei area.

(2) Fault–Fracture Type

The fault–fracture tectonic style is characterized by the largest number of fractures, mainly including inclined fractures and high-angle fractures, with most of them being open-to-semi-open fractures. The fracture development in this tectonic style is significantly controlled by 2–3-grade faults. The closer the distance to the fault, the greater the number

of fractures. This is because fault activities create stress-concentrated areas nearby, causing the rocks to rupture and form fractures (Figure 6). Fractures are more developed in thin sandstone layers of conglomeratic coarse sandstone and glutenite. These thin, coarse-grained sandstone layers can more easily accumulate energy and rupture during the stress transfer process, thus forming a large number of fractures. For example, well locations, such as YN 2 and DB 5, which are within the area of this tectonic style, have a high degree of fracture development, fully demonstrating the controlling effect of the fault–fracture tectonic style on fracture distribution.

(3) Monocline Type

In the monocline tectonic style, due to the lack of influence of fault–fold actions, overall fracture development is scarce. Compared with the fault–fold–fracture and fault–fracture tectonic styles, the strata in the monocline tectonic style are relatively stable, lacking sufficient tectonic stress to promote the formation of large-scale fractures. Therefore, the number of fractures is small (Figure 6). Well locations, such as DB 6 and DB 102, which are in this tectonic style area, have significantly poor fracture development, conforming to the fracture distribution characteristics of the monocline tectonic style.

In summary, the fracture distribution models of the tight reservoirs in the Ahe Formation of the Dibei area exhibit distinct characteristics under different tectonic styles. Tectonic styles and lithology interact with each other, jointly determining the types, numbers, and spatial distributions of fractures. A thorough understanding of the fracture distribution model helps to accurately evaluate the quality of reservoirs and the potential for oil and gas exploration and development, providing a scientific basis for formulating rational exploration and development plans.

4. Discussion

4.1. The Control Mechanism of Folds on the Development of Natural Fractures

Folds play a crucial controlling role in the development of natural fractures in the tight reservoirs of the Ahe Formation in the Dibei area of the Tarim Basin [48]. Based on actual geological data, the strata rocks in the folded areas are subjected to intense compression and deformation, leading to stress concentration within the rocks and the development of high-angle open fractures (Figure 7). Taking Well DT 2 as an example, there is a significant difference in fracture development between its folded and non-folded parts. The rocks in the folded part undergo bending deformation under tectonic stress, and the weak planes within the rocks are stretched and ruptured, resulting in the formation of numerous high-angle open fractures. In contrast, in the non-folded part, the overall tectonic stress is relatively weak, the degree of rock deformation is low, and the fracture development is poor.

Further analysis of the imaging logging data from multiple wells in the region reveals that there are also differences in the fracture development characteristics between the high and low parts of the folds. The high part of the fold is the core area of stress concentration, where the rocks are subjected to the most intense stress, and the fracture density and aperture are relatively large [49]. In this area, most fractures intersect the axial plane of the high part of the fold vertically or at high angles. These fractures provide excellent channels and spaces for the migration and storage of oil and gas. Although the fracture development degree in the low part of the fold is relatively poor, it is still more developed compared to non-folded areas. Moreover, the occurrence of fractures in the low-part of the fold is influenced by fold deformation, showing a certain regular distribution (Figure 7). The tightness and scale of the folds also affect fracture development. Tight folds, compared with open folds, have more concentrated internal stress and more intense rock deformation,

which is more conducive to the formation and expansion of fractures. Therefore, the fracture density and effectiveness in tight folds are higher [49]. Larger-scale folds have a wide influence range, which can provide more power and space for fracture development over a larger area, making the fractures in the surrounding strata more extensive and complex.

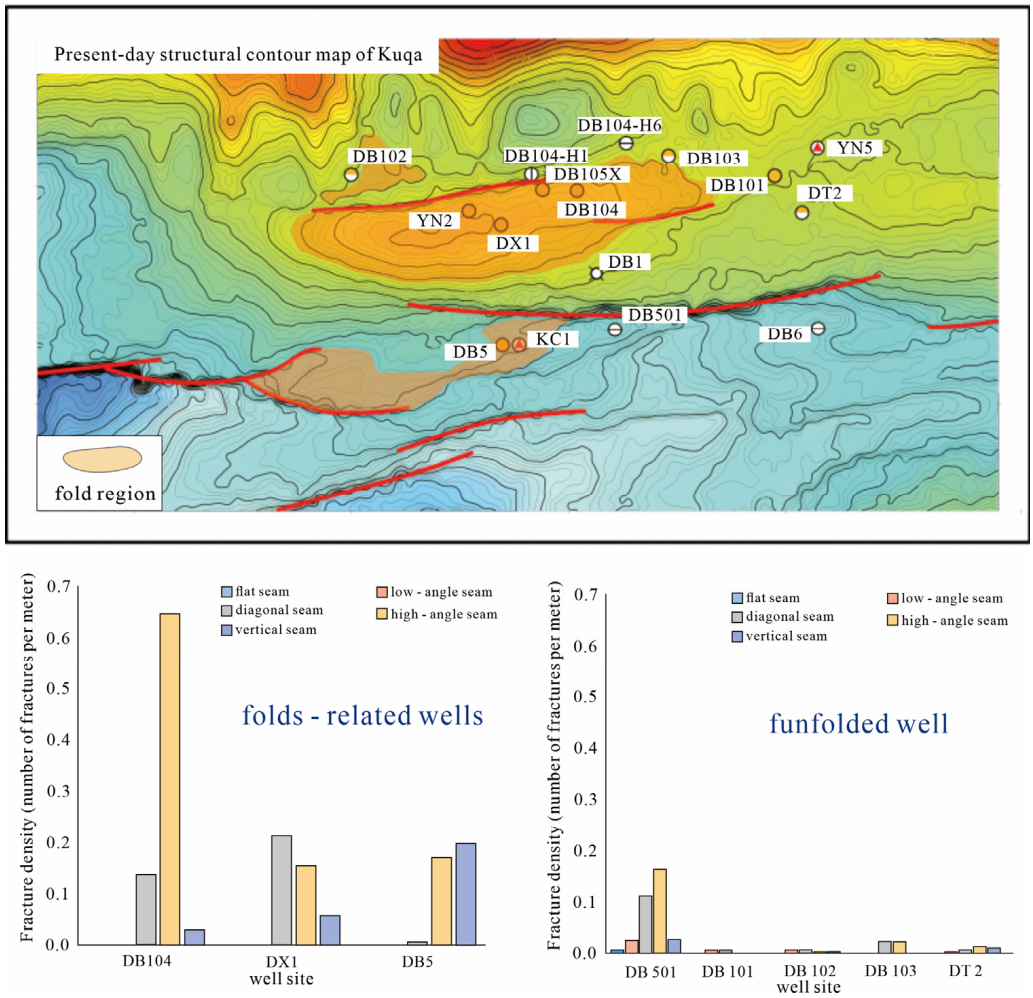


Figure 7. Kuqa—present tectonic contour map of the Dibei area.

In summary, folds, as an important controlling factor in the development of natural fractures in the tight reservoirs of the Ahe Formation in the Dibei area, affect the development degree, occurrence, and distribution characteristics of fractures by changing the internal stress state of the rocks. High-angle and open fractures are more developed in the high part of the folds. In-depth study of the relationship between folds and fractures is of great significance for accurately predicting the distribution of reservoir fractures and evaluating the potential of oil and gas exploration and development.

4.2. The Control Mechanism of Faults on the Development of Natural Fractures

Fault activity represents a pivotal controlling factor in the development of natural fractures within the tight reservoirs of the Ahe Formation in the Dibei area of the Tarim Basin [50]. The faulting events in this region are characterized by multi-episodicity and variability, with faults of varying activity intensities exerting disparate controls on fracture development [51]. Proximal to moderately and strongly active faults, fractures tend to be more prolific, whereas the degree of fracture development adjacent to weakly active faults is markedly lower (Figure 8).

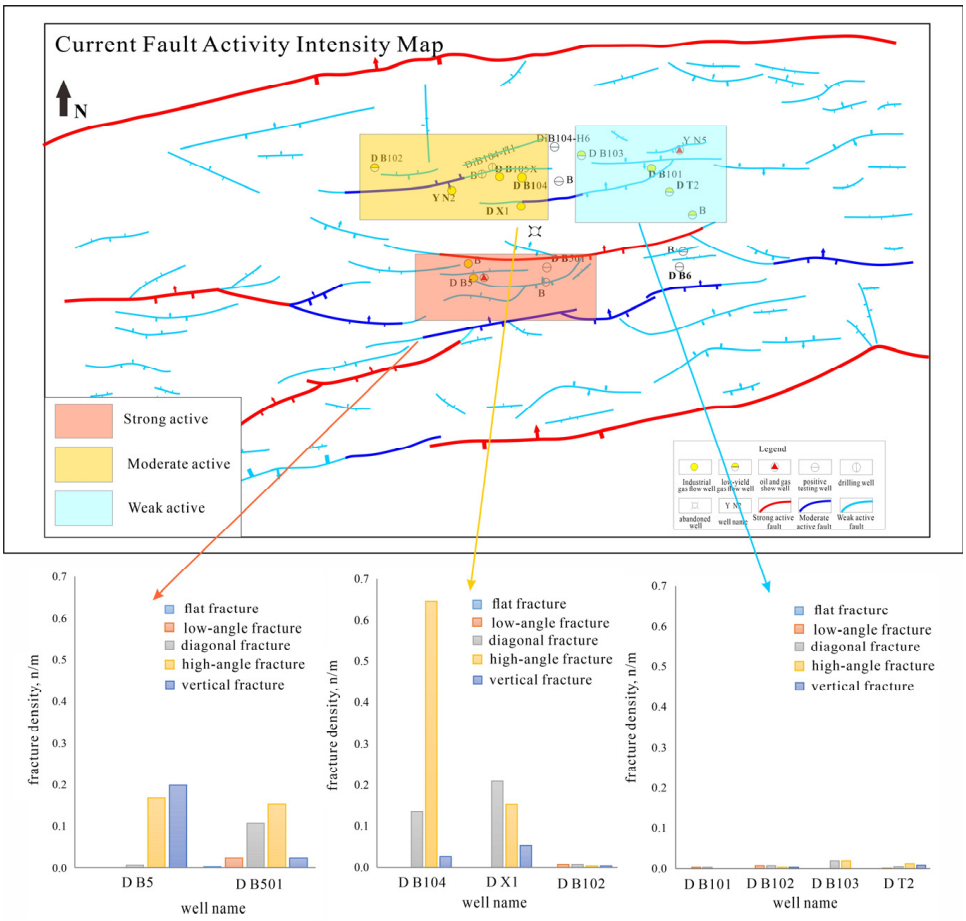


Figure 8. Late Cenozoic fault activity map of the Dibei area.

For example, during the activation of a strongly active fault, substantial displacement and friction occur. These processes cause the rocks surrounding the fault to fracture, giving rise to a multitude of fractures. These fractures are not only abundant in number but also possess relatively large apertures and favorable connectivity, thereby creating propitious conditions for the migration and accumulation of oil and gas. By integrating the current fault activity map with imaging logging data from diverse wells in the Dibei area, it becomes evident that the fracture density in the vicinity of strongly active faults is significantly higher than that near weakly active faults. For both strongly active and moderately active faults, a closer proximity to the fault corresponds to more favorable fracture development. This phenomenon can be attributed to the fact that rocks in the vicinity of the fault are subjected to more intense stress. In stress-concentrated zones, the internal granular structure of the rock is disrupted, leading to the formation of numerous fractures. Additionally, fault activity may trigger geological events, like earthquakes, which further contribute to rock fracturing, augmenting the number and scale of fracture [52]. For instance, when a fault experiences displacement, the surrounding rocks are subjected to additional impact forces. This disrupts the original intact rock structure, generating new fractures and facilitating the further propagation of existing fractures [53].

For highly active faults, the closer the distance to the fault, the better the degree of fracture development. This is because rocks near the fault are subjected to more intense stress, making them more prone to rupture. In stress-concentrated regions, the internal particle structure of the rocks is damaged, leading to the formation of numerous fractures. Moreover, fault activities may trigger geological events, such as earthquakes, which further contribute to rock fracturing and increase the number and scale of fractures.

4.3. The Control Mechanism of Lithology on the Development of Natural Fractures

Lithologic combinations significantly influence the development of natural fractures in the tight reservoirs of the Ahe Formation in the Dibei area of the Tarim Basin [54] (Figure 9). In the Dibei area, homogeneous sandstone and sand–mud interbeds represent two typical lithologic assemblages, each with unique petrophysical properties and structural characteristics, thereby resulting in marked disparities in fracture development.

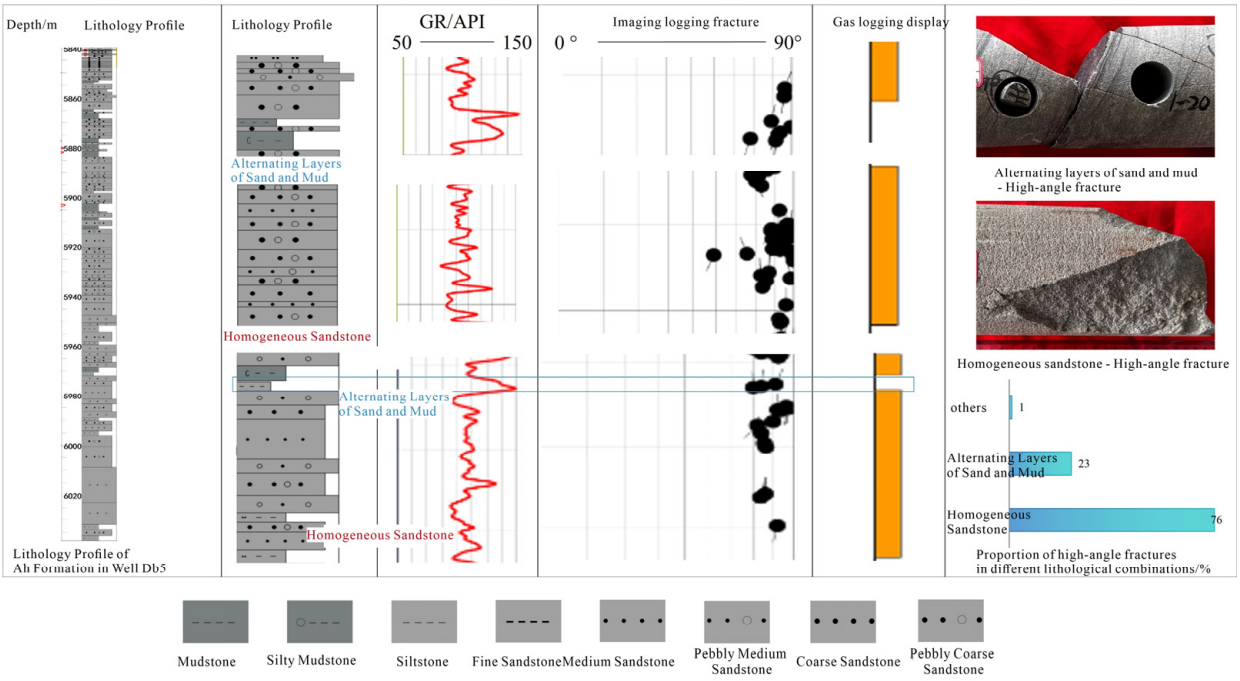


Figure 9. Proportions of tectonic fractures in different lithologic assemblages of Well DB 5 in the Dibei area.

Homogeneous sandstone, defined as a massive sandstone with a monolayer thickness exceeding 2 m, stable mineral composition (quartz content > 75%), excellent grain sorting (sorting coefficient < 1.5), and uniformly distributed cement, serves as a prime interval for the development of high-angle fractures [55]. The homogeneity of this lithologic combination endows it with relatively consistent mechanical properties. Under the action of tectonic stress, stress can be efficiently transmitted and accumulated. Once the stress reaches the rock's failure strength, the rock is predisposed to generate high-angle fractures. For example, in Well DB 104, situated in the elevated portion of the fault block zone, the fracture density within its homogeneous sandstone interval reaches 0.809 fractures per meter (Table 3), with high-angle fractures showing a concentrated development pattern. Similarly, in Well DX 1, the fracture density in the homogeneous sandstone interval is 0.419 fractures per meter, predominantly composed of high-angle fractures. This clearly indicates that homogeneous sandstone provides favorable material and mechanical bases for the formation of high-angle fractures.

In sand–mud interbeds, the presence of mudstone mitigates fracture development. Mudstone, with its high plasticity, can undergo plastic deformation under tectonic stress. This deformation enables it to absorb and disperse a portion of the stress, thereby reducing the stress concentration within the sandstone and leading to relatively subdued fracture development [56]. Taking the sand–mud interbed interval of Well DB 5 as an example, its fracture density is 0.372 fractures per meter (Table 3), featuring bedding fractures, inclined fractures, and some high-angle fractures. Overall, the fracture development intensity in this interval is lower than that in homogeneous sandstone intervals. Additionally, the interface

between mudstone and sandstone in sand–mud interbeds is a crucial factor influencing fracture development. Due to the discrepancies in mechanical parameters, such as the elastic modulus and Poisson's ratio between mudstone and sandstone, stress concentration readily occurs at the interface under tectonic stress, facilitating the preferential development of fractures in the vicinity [57]. Nevertheless, the buffering effect of mudstone imposes certain constraints on the propagation and expansion of these fractures.

Table 3. Development of structural fractures in different lithology combinations.

Regional Distribution		Well Name	Lithologic Combination	Fracture Development Status			
				(Semi-) Open Fracture	Closed Fracture	Tectonic Fractures	Density
Fault terrace zone area	High position of the fault terrace zone	DX1	Sand–mud interbed	0.081	0.03	0.111	0.111
			Homogeneous sandstone	0.295	0.004	0.299	0.299
	Low position of the fault terrace zone	DB 102	Sand–mud interbed		0.007	0.007	0.007
			Homogeneous sandstone		0.011	0.011	0.011
Southern slope	High position of the southern slope	**DB 5**	Sand–mud interbed	0.111		0.111	0.111
			Homogeneous sandstone	0.256		0.256	0.256
	Low position of the southern slope	**DB 501**	Sand–mud interbed	0.221	0.009	0.227	0.23
			Homogeneous sandstone	0.095	0.003	0.084	0.098

From a microscopic perspective, due to its compositional and structural characteristics, the sandstone of the Ahe Formation in the Dibei area generally exhibits strong brittleness. The quartz grains in the rock are of high hardness and are evenly distributed, and the cement fills the spaces between the grains, resulting in a relatively compact overall structure. When subjected to tectonic stress, the relative displacement and dislocation among grains are more likely to trigger overall rupture, giving rise to high-angle fractures [38] (Figure 10a–c). This is because the mechanical properties of homogeneous sandstone are uniform, facilitating smooth stress transfer. In stress-concentrated areas, the rock is more prone to rupture along vertical or nearly vertical directions.

In sand–mud interbeds, however, the fine-grained structure and plastic characteristics of mudstone render it difficult for large-scale fractures to form within the mudstone itself (Figure 10d). Moreover, mudstone impedes the propagation of fractures in sandstone. Under stress, mudstone undergoes plastic deformation and absorbs part of the stress, causing fractures in sand–mud interbeds to be predominantly low-angle and bedding fractures, with relatively fewer high-angle fractures. Certain minerals, such as feldspar and lithic fragments, due to their relatively poor chemical stability during long-term geological processes, are prone to dissolution and alteration. This further reduces the overall strength of the rock, making it more susceptible to fracturing when subjected to stress [58] (Figure 10e,f). Lithologic combinations exert a significant influence on the development degree, occurrence, and distribution of natural fractures in the tight reservoirs of the Ahe Formation in the Dibei area. Homogeneous sandstone is conducive to the development of high-angle fractures, while sand–mud interbeds, due to the buffering effect of mudstone, experience a lower degree of fracture development and have a greater variety of fracture types.

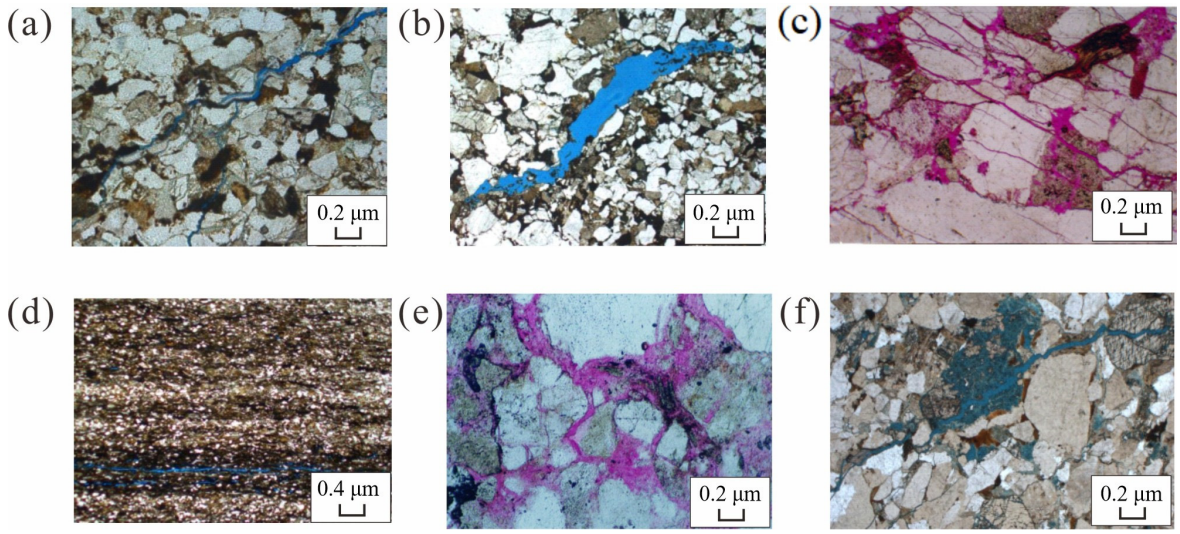


Figure 10. Microscopic cast thin-section photographs of rocks: (**a**) Well DT2, at a depth of 5112.73 m, showing tectonic fractures; (**b**) Well DT2, at a depth of 5124.04 m, showing tectonic fractures; (**c**) Well YN5, at a depth of 4846.29 m, showing tectonic fractures; (**d**) Well DT2, at a depth of 5105.51 m, showing bedding fractures; (**e**) Well YN2, at a depth of 4843.01 m, showing feldspar dissolution fractures; (**f**) Well DB5, at a depth of 5845.9 m, showing feldspar dissolution fractures.

4.4. The Control Mechanism of Stress on the Development of Natural Fractures

Stress is one of the crucial factors influencing the development of natural fractures in the tight reservoirs of the Ahe Formation in the Dibei area of the Tarim Basin [59]. It significantly affects the opening, closing, and development degree of fractures. Against the complex geological tectonic background of the Dibei area, multiple tectonic movements have superimposed, subjecting the strata rocks to various stress actions and, thus, forming the diverse fracture systems observed today.

Based on the analysis of the regional stress field, the angle between the dominant strike of fractures and the direction of in situ stress plays a key role in controlling the opening and closing states of fractures [60]. When this angle ranges from 0° to 30°, fractures are more likely to open (Figure 11 and Table 3). Within this angular range, the in-situ stress can effectively act on the fracture surface, promoting fracture opening and increasing fracture aperture and connectivity [61]. For example, Well DX1 and Well DB 104, located at the high part of the fault block zone, have the dominant strike of their fractures mostly at an angle of 0– 30° with the in situ stress. The density of open fractures in Well DX 1 reaches 0.376 fractures per meter, and that in Well DB 104 is 0.809 fractures per meter. High-angle fractures in these wells are well-developed, providing favorable channels for the seepage of oil and gas. Conversely, when the angle between the dominant strike of fractures and the in situ stress exceeds 45°, fractures tend to close. This is because a larger angle makes the force exerted by the in situ stress on the fracture surface less conducive to maintaining the open state of the fracture. The mutual extrusion between rock grains intensifies, resulting in a reduction in the fracture aperture or even complete closure [62–64]. Take Well DB 102, located at the low part of the fault block zone, as an example. The dominant strike of some of its fractures has an angle close to 90° with the in-situ stress. Its fracture density is only 0.021 fractures per meter, and most of the fractures are closed, which severely affects the storage and migration of oil and gas.

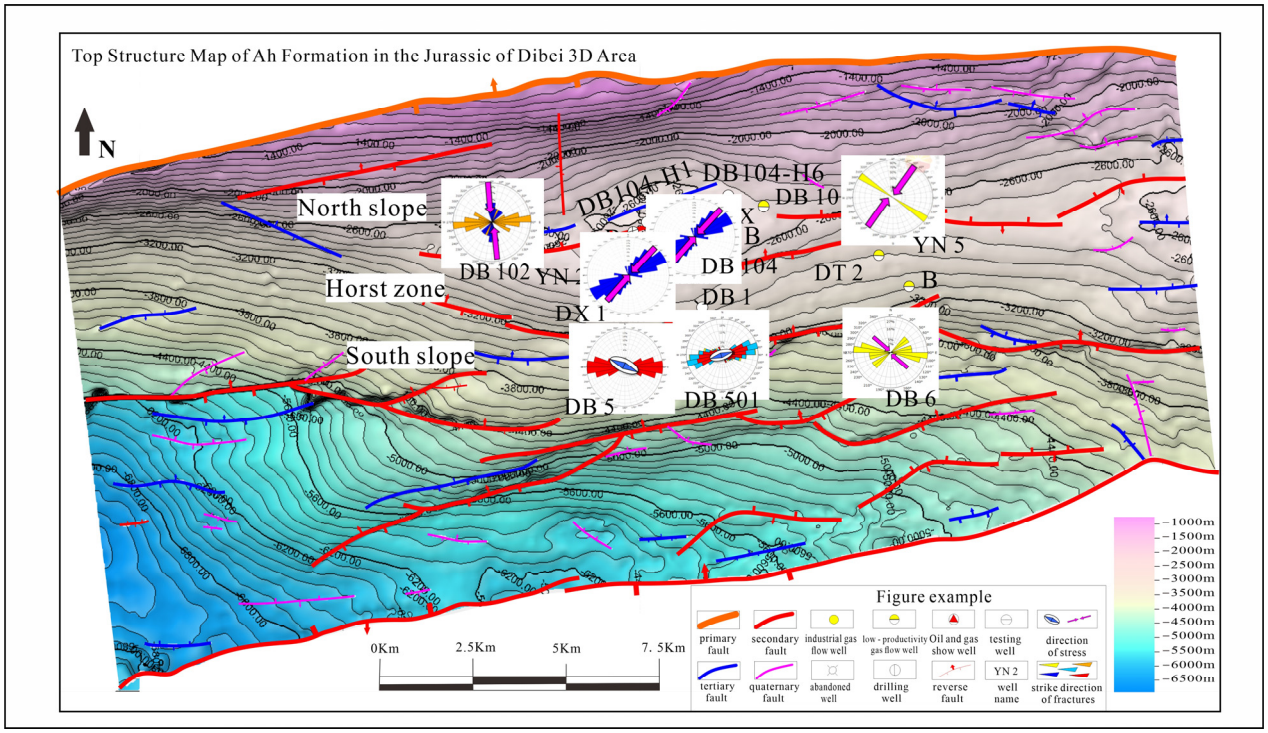


Figure 11. Planar distribution of the angle between the dominant strike of fractures and the ground stress in the Ahe Formation of the Dibei area.

In summary, our analysis reveals that although the overall fracture density in the study area follows the pattern of "high parts of the horst zone > southern slope > low parts of the horst zone", some regions exhibit fracture density anomalies inconsistent with expectations in actual observations. Such uncertainties mainly stem from the complexity of geological conditions and deviations caused by the coupling effect of multiple factors. For instance, Well DX1 is located in the high part of the horst zone, while Well DB5 is situated on the southern slope, yet their overall fracture development degrees are comparable, with the vertical fracture density of Well DX1 being lower than that of Well DB5. Based on the above analysis, it can be concluded that both Well DB5 and Well DX1 are located in fold zones, where stress is more concentrated than in other areas. Meanwhile, Well DB5 is near a strongly active fault, with more intense faulting activity than Well DX1. Additionally, the reservoir lithology of Well DB5 is mostly homogeneous sandstone, accounting for 76%, which is highly prone to developing high-angle tectonic fractures. Thus, despite being on the southern slope, Well DB5 exhibits a tectonic fracture development degree comparable to that of Well DX1 in the horst zone.

4.5. Geological Significance

In the study of natural fractures within the tight reservoirs of the Ahe Formation in the Dibei area, three key new insights have been derived, offering valuable guidance for future exploration, modeling, and seismic analysis.

First, our study reveals the differential control of structural styles on fracture systems; specifically, the fault–fold–fracture type develops the most complex fracture networks due to the synergistic effect of fold compression and reverse faulting, whereas the monocline type, constrained by weak stress, exhibits minimal fracture development. This precise differentiation of structural fracture coupling mechanisms fills the gap in fine-scale fracture distribution modeling under various microstructural units. Second, the study clarifies the controlling effect of lithology: homogeneous sandstones promote high-angle fracture

development by concentrating tectonic stress, while sand–mud interbeds inhibit fracture propagation through the plastic buffering effect of mudstones. The promotional effect of homogeneous sandstones on high-angle fracture development and the inhibitory mechanism of sand–mud interbeds on fracture propagation serve as core training samples in the lithological input layer of machine learning models [65], enabling algorithms to more accurately capture the intrinsic lithology–fracture correlation. Finally, the study identifies the critical stress–fracture angle threshold (0–30°) for fracture initiation, providing reasonable constraints for prediction models and improving accuracy in forecasting fracture effectiveness—particularly those controlling hydrocarbon migration. These quantitative indicators enrich input features of machine learning models, enhance correlation between predictions and geological reality [26], and offer a solid geological basis for subsequent fracture prediction modeling.

These insights hold significant implications for future work: For exploration, prioritizing fault–fold zones with homogeneous sandstones and stress–fracture angles <30° can optimize sweet-spot targeting. In modeling, integrating structural style–lithology–stress coupling mechanisms will enhance predictive accuracy of fracture networks. For seismic analysis, developing dedicated attributes (e.g., lithology-sensitive inversion for homogeneous sandstones, and stress field modeling for angle detection) could improve subsurface fracture characterization in similar tight reservoir settings.

5. Conclusions

This study systematically investigates the characteristics, distribution patterns, and controlling factors of natural fractures in the tight reservoirs of the Ahe Formation in the Dibei area, Tarim Basin, using integrated methods, including core observation, imaging logging analysis, and thin-section microscopy. The research clarifies the dominant genetic types of fractures, their spatial variability, and the key geological factors governing their development, providing critical insights into hydrocarbon migration and accumulation mechanisms in tight sandstone systems. The primary conclusions are as follows:

(1) In the tight reservoirs of the Ahe Formation in the Dibei area of the Tarim Basin, the natural fractures are mainly of tectonic and sedimentary origins, with the tectonic origin being dominant, which is related to multiple tectonic movements. Morphologically, they are dominated by high-angle and open fractures, facilitating the storage and migration of oil and gas. Planar-wise, the high part of the fault block zone has the highest fracture density, being significantly influenced by tectonic stress. The fracture strikes are divided into three systems, namely nearly EW-trending, NE-trending, and nearly SN-trending. The nearly EW-trending fractures are the most widespread, and high-angle fractures are dominant.

(2) In the fault–fold–fracture type, the activities of folds and reverse faults provide the driving force and space for fracture formation. The fault–fracture type is controlled by 2–3-grade faults, with more fractures in favorable rock layers. In the monocline type, due to the stable structure and weak stress, fracture development is scarce. Overall, in the study area, the fault–fold–fracture type has the most fractures, followed by the fault–fracture type, and the monocline type has the least.

(3) The development of natural fractures in the tight reservoirs of the Ahe Formation in the Dibei area is jointly controlled by multiple factors. In the high part of the fold, stress is concentrated, which is conducive to the formation of high-angle open fractures. Fractures are more developed near moderately and strongly active faults, and the closer to the fault, the more obvious this is. When the angle between the stress and the fracture strike is between 0–30°, the fractures are likely to open, facilitating oil

and gas migration. Homogeneous sandstone is more conducive to the development of high-angle fractures compared to sand–mud interbeds.

Author Contributions: Conceptualization, Y.W. and H.P.; Data curation, J.J. and L.S.; Formal analysis, T.Z. and L.L.; Funding acquisition, H.P. and D.C.; Investigation, C.Z. and J.D.; Methodology, Y.T., L.Z. and J.J.; Project administration, Y.T. and L.Z.; Resources, Y.T., L.Z. and J.J.; Software, L.S. and G.Z.; Supervision, Y.W. and H.P.; Validation, Y.T., Y.W. and H.P.; Visualization, S.L. and D.C.; Writing—original draft, Y.T.; Writing—review and editing, Y.W., H.P. and D.C. All authors have read and agreed to the published version of the manuscript.

Funding: This research received no external funding.

Data Availability Statement: The original contributions presented in this study are included in the article. Further inquiries can be directed to the corresponding authors.

Conflicts of Interest: Authors Yangang Tang, Liang Zhang, Jun Jiang, Lin Shen, Guowei Zhang, Tiantian Zhao, Ling Li, Chang Zhou and Jianzhong Deng were employed by the Tarim Oilfield Company, China National Petroleum Corporation. The remaining authors declare that the research was conducted in the absence of any commercial or financial relationships that could be construed as a potential conflict of interest. All authors have read and agreed to the published version of the manuscript.

References

1. Wang, P.; Cui, Y.A.; Liu, J.X. Fluid Discrimination Based on Inclusion-Based Method for Tight Sandstone Reservoirs. *Surv. Geophys.* **2022**, *43*, 1469–1496. [CrossRef]
2. Aqsa, A.; Zhang, H.C.; Umar, A.; Wang, R.; Thanh, H.T.; Radwan, A.E.; Ullah, J.; Abbasi, G.R.; Iqbal, I.; Naffees, A.; et al. Sand-ratio distribution in an unconventional tight sandstone reservoir of Hangjinqi area, Ordos Basin: Acoustic impedance inversion-based reservoir quality prediction. *Front. Earth Sci.* **2022**, *10*, 1018105.
3. Gao, H.; Li, A.H. Pore structure characterization, permeability evaluation and enhanced gas recovery techniques of tight gas sandstones. *J. Nat. Gas Sci. Eng.* **2016**, *28*, 536–547. [CrossRef]
4. Shi, J.X.; Zhao, X.Y.; Zhang, Y.Z.; You, Y.C.; Shang, M.H.; Zhu, Z.P. Characteristics and Controlling Factors of Natural Fractures in Deep Carbonates of the Puguang Area, Sichuan Basin, China. *ACS Omega* **2024**, *9*, 16071–16083. [CrossRef]
5. Du, X.Y.; Jin, Z.J.; Zeng, L.B.; Liu, G.P.; He, W.J.; Mehdi, O.; Liang, X.P.; Yang, S.; Lu, G.P. Characteristics and controlling factors of natural fractures in deep lacustrine shale oil reservoirs of the Permian Fengcheng Formation in the Mahu Sag, Junggar Basin, China. *J. Struct. Geol.* **2023**, *175*, 104923. [CrossRef]
6. Zhao, S.F.; Chen, W.; Wang, Z.H.; Li, T.; Wei, H.X.; Ye, Y. Fluid geochemistry of the Jurassic Ahe Formation and implications for reservoir formation in the Dibei area, Tarim Basin, northwest China. *Energy Explor. Exploit.* **2018**, *36*, 801–819. [CrossRef]
7. Tang, Y.G.; Yang, X.Z.; Xie, H.W. Tight gas reservoir characteristics and exploration potential of Jurassic Ahe Formation in Kuqa depression, Tarim Basin. *China Pet. Explor.* **2021**, *26*, 113–124.
8. Zhang, R.H.; Zeng, Q.L.; Wang, K. New progress in the theory and technology of tectonic diagenesis on reservoir and the geological significance of ultra-deep oil and gas exploration. *Acta Pet. Sin.* **2020**, *41*, 1278–1292.
9. Li, H.; Liu, Y.; Wang, S.; Xi, K.L.; Yang, X.Z.; Yu, G.D. Mesozoic Tectonic Setting and Evolution in Kuqa Depression of the Tarim Basin: A Study of Detrital Zircons and Geochemistry. *ACS Omega* **2025**, *10*, 13193–13208. [CrossRef]
10. Yang, K.J.; Xu, L.W.; Qi, J.F.; He, P.; Du, J.M.; Sun, T. Structural deformation of the Northern Monocline belt in the Kuqa depression and implications for the Cenozoic uplift history of the South Tianshan Mountains. *Tectonophysics* **2023**, *857*, 229840. [CrossRef]
11. Zhao, G.J.; Li, X.Q.; Liu, M.C.; Dong, C.Y.; Chen, D.Y.; Zhang, J.Z. Reservoir Characteristics of Tight Sandstone and Sweet Spot Prediction of Dibei Gas Field in Eastern Kuqa Depression, Northwest China. *Energies* **2022**, *15*, 3135. [CrossRef]
12. Li, J.; Hu, D.F.; Zou, H.Y.; Shang, X.Q.; Ren, H.J.; Wang, L.C. Coupling relationship between reservoir diagenesis and gas accumulation in Xujiahe Formation of Yuanba–Tongnanba area, Sichuan Basin. *China. J. Nat. Gas Geosci.* **2016**, *5*, 335–352. [CrossRef]
13. Wang, Q.H.; Zhang, R.H.; Yang, X.Z. Major Breakthroughs in the Exploration of Tight Sandstone Gas in the Jurassic Ahe Formation in the Dibei Area, Eastern Kuqa Depression and Their Geological Significance. *Acta Pet. Sin.* **2022**, *43*, 1049–1064.
14. Jiang, Z.X.; Li, F.; Yang, H.J.; Li, Z.; Liu, L.F.; Chen, L.; Du, Z.M. Development characteristics of fractures in Jurassic tight reservoir in Dibei area of Kuqa depression and its reservoir-controlling mode. *Acta Pet. Sin.* **2015**, *36*, 102–111.

15. Shi, C.Q.; Li, Y.; Yuan, W.F.; Jiang, J.; Xie, Y.N.; Zhang, R.H.; Zhou, S.Y.; Lou, H.; Wang, Z.T.; Zhang, H.F.; et al. Characteristics on reservoir architecture and quality of tight sandstone reservoirs: Taking Jurassic Ahe formation in Dibei area of Kuqa foreland basin as an example. *J. China Univ. Min. Technol.* **2021**, *50*, 877–892.
16. Lu, H.; Lu, X.S.; Fan, J.J.; Zhao, M.J.; Wei, H.X.; Zhang, B.S.; Lu, Y.H. Controlling effect of fractures on gas accumulation and production within the tight sandstone: A case study on the Jurassic Dibei gas reservoir in the eastern part of the Kuqa foreland basin, China. *J. Nat. Gas Geosci.* **2016**, *1*, 61–71. [CrossRef]
17. Dong, C.Y.; Yang, W.; Li, J.; Li, D.J.; Wu, X.Q.; Miao, W.D.; Zhu, H.H.; Yang, X.L. Lower limits of physical properties and classification evaluation criteria of the tight reservoir in the Ahe Formation in the Dibei Area of the Kuqa depression. *Open Geosci.* **2024**, *16*, 20220572. [CrossRef]
18. Wei, G.Q.; Wang, K.; Zhang, R.H.; Wang, B.; Yu, C.F. Structural diagenesis and high-quality reservoir prediction of tight sandstones: A case study of the Jurassic Ahe Formation of the Dibei gas reservoir, Kuqa depression, Tarim basin, NW China. *J. Asian Earth Sci.* **2022**, *239*, 105399. [CrossRef]
19. Wei, X.; Liu, K.; Yang, X.; Liu, J.L.; Zhou, L.; Ding, X.J. Probing Petroleum Sources Using Geochemistry, Multivariate Analysis, and Basin Modeling: A Case Study from the Dibei Gas Field in the Northern Kuqa Foreland Basin, NW China. *Appl. Sci.* **2025**, *15*, 2425. [CrossRef]
20. Wei, J.; Wang, K. A preliminary study of the present-day in-situ stress state in the Ahe tight gas reservoir, Dibei Gasfield, Kuqa Depression. *Mar. Pet. Geol.* **2018**, *96*, 154–165.
21. Wang, K.; Xiao, A.C.; Cao, T.; Zhang, R.H.; Wei, H.X.; Yu, C.F. Geological structures and petroleum exploration fields of the northern tectonic belt in the Kuqa depression, Tarim basin. *Acta Geol. Sin.* **2022**, *96*, 368–386.
22. Yu, G.D.; Yuan, J.; Liu, K.Y.; Yang, X.Z.; Dong, D.T.; Ma, P.J.; Huang, C.Q. Diagenesis of the Paleogene Sandstones in the DN2 Gas Field, Kuqa Foreland Basin and its Link to Tectonics. *Acta Geol. Sin.* **2023**, *97*, 1538–1554. [CrossRef]
23. Pang, X.Q.; Peng, J.W.; Jiang, Z.X.; Yang, H.J.; Wang, P.W.; Jiang, F.J.; Wang, K. Hydrocarbon accumulation processes and mechanisms in Lower Jurassic tight sandstone reservoirs in the Kuqa subbasin, Tarim Basin, northwest China: A case study of the Dibei tight gas field. *AAPG Bull.* **2019**, *103*, 769–796. [CrossRef]
24. Cai, M.L.Y.; Li, M.; Zhu, X.S.; Luo, H.; Zhang, Q. Comprehensive Evaluation of Rock Mechanical Properties and in-situ Stress in Tight Sandstone Oil Reservoirs. *Front. Earth Sci.* **2022**, *10*, 911504. [CrossRef]
25. Wang, X.J.; Jin, Z.J.; Chen, G.; Peng, M.; Huang, L.L.; Wang, Z.L.; Zeng, L.B.; Lu, G.Q.; Du, X.Y.; Liu, G.P. Multi-Scale Natural Fracture Prediction in Continental Shale Oil Reservoirs: A Case Study of the Fengcheng Formation in the Mahu Sag, Junggar Basin, China. *Front. Earth Sci.* **2022**, *10*, 929467. [CrossRef]
26. Somayeh, T.; Pezhman, S.T.; Meysam, R.; David, A.W.; Shadfar, D.; Hamzeh, G.; Nima, M.; Mehdi, A.A. Optimized machine learning models for natural fractures prediction using conventional well logs. *Fuel* **2022**, *326*, 124952. [CrossRef]
27. Shen, Y.Q.; Lv, X.X.; Guo, S.; Song, X.; Zhao, J. Effective evaluation of gas migration in deep and ultra-deep tight sandstone reservoirs of Keshen structural belt, Kuqa depression. *J. Nat. Gas Sci. Eng.* **2017**, *46*, 119–131. [CrossRef]
28. Zeng, J.H.; Zhang, Y.C.; Zhang, S.W.; Qiao, J.C.; Feng, X.; Feng, S. Experimental and theoretical characterization of the natural gas migration and accumulation mechanism in low-permeability (tight) sandstone cores. *J. Nat. Gas Sci. Eng.* **2016**, *33*, 1308–1315. [CrossRef]
29. Li, J.; Li, X.R.; Song, M.S.; Liu, H.M.; Feng, Y.C.; Liu, C. Investigating microscopic seepage characteristics and fracture effectiveness of tight sandstones: A digital core approach. *Pet. Sci.* **2021**, *18*, 173–182. [CrossRef]
30. Xiao, L.; Li, J.R.; Mao, Z.Q.; Yu, H.Y. A method to evaluate pore structures of fractured tight sandstone reservoirs using borehole electrical image logging. *AAPG Bull.* **2020**, *104*, 205–226. [CrossRef]
31. Lyu, W.Y.; Zeng, L.B.; Liao, Z.H.; Ji, Y.Y.; Lyu, P.; Dong, S.Q. Fault damage zone characterization in tight-oil sandstones of the Upper Triassic Yanchang Formation in the southwest Ordos Basin, China: Integrating cores, image logs, and conventional logs. *Interpretation* **2017**, *5*, SP27–SP39. [CrossRef]
32. Liu, H.; Ren, Y.L.; Li, X.; Hu, Y.X.; Wu, J.P.; Li, B.; Luo, L.; Tao, Z.; Liu, X.; Liang, J.; et al. Rock thin-section analysis and identification based on artificial intelligent technique. *Pet. Sci.* **2022**, *19*, 1605–1621. [CrossRef]
33. Xu, Z.H.; Ma, W.; Lin, P.; Hua, Y.L. Deep learning of rock microscopic images for intelligent lithology identification: Neural network comparison and selection. *J. Rock Mech. Geotech. Eng.* **2022**, *14*, 1140–1152. [CrossRef]
34. Rashid, F.; Hussein, D.; Lawrence, J.A.; Khanaqa, P. Characterization and impact on reservoir quality of fractures in the Cretaceous Qamchuqa Formation, Zagros folded belt. *Mar. Pet. Geol.* **2020**, *113*, 104117. [CrossRef]
35. Zeng, L.B.; Song, Y.C.; Liu, G.P.; Tan, X.L.; Xu, X.T.; Yao, Y.T.; Mao, Z. Natural fractures in ultra-deep reservoirs of China: A review. *J. Struct. Geol.* **2023**, *175*, 104954. [CrossRef]
36. Gong, L.; Su, X.C.; Gao, S.; Fu, X.F.; Jabbari, H.; Wang, X.X.; Liu, B.; Yue, W.T.; Wang, Z.S.; Gao, A. Characteristics and formation mechanism of natural fractures in the tight gas sandstones of Jiulongshan gas field, China. *J. Pet. Sci. Eng.* **2019**, *175*, 1112–1121. [CrossRef]

37. Zeng, L.B.; Gong, L.; Zhang, Y.Z.; Dong, S.Q.; Lyu, W.Y. A review of the genesis, evolution, and prediction of natural fractures in deep tight sandstones of China. *AAPG Bull.* **2023**, *107*, 1687–1721. [CrossRef]
38. Wu, H.; Kong, X. Fine description of natural fractures in the tight sandstone reservoir of the Yanchang reservoirs in the southern Ordos Basin. *Sci. Rep.* **2025**, *15*, 6152. [CrossRef]
39. Li, Y.; Guo, S.; Wang, X.; Hou, Y.F.; Neng, Y.; Wang, Z.X.; Zhou, L.; Yang, W.J.; Tan, C. Stratification model of an ultra-deep tight sandstone fracture reservoir under tectonic stress: A case study of a Cretaceous reservoir in the Kuqa foreland thrust belt of the Tarim Basin. *J. Nat. Gas Sci. Eng.* **2017**, *45*, 53–64. [CrossRef]
40. Zeng, L.B. Microfracturing in the Upper Triassic Sichuan Basin tight-gas sandstones: Tectonic, overpressure, and diagenetic origins. *AAPG Bull.* **2010**, *94*, 1811–1825. [CrossRef]
41. Yin, S.; Tian, T.; Wu, Z.H. Developmental characteristics and distribution law of fractures in a tight sandstone reservoir in a low-amplitude tectonic zone, eastern Ordos Basin, China. *Geol. J.* **2020**, *55*, 1546–1562. [CrossRef]
42. Wang, Z.M.; Wang, C.L.; Xu, K.; Zhang, H.; Chen, N.D.; Deng, H.C.; Hu, X.F.; Yang, Y.Y.; Feng, X.S.; Du, Y.; et al. Development Characteristics and Controlling Factors of Tectonic Fractures in Ultra—Deep Tight Sandstones: A Case Study of the Lower Cretaceous Reservoirs in the Bozhi—Dabei Area, Kuqa Depression, Tarim Basin. *Nat. Gas Geosci.* **2023**, *34*, 1535–1551.
43. Xu, K.; Yang, H.J.; Zhang, H.; Zhao, B.; Yin, G.Q.; Wang, Z.M.; Wang, H.Y. High—Efficiency Exploration Technology for Deep Tight Gas Reservoirs Based on Geomechanical Methods: A Case Study of the Dibei Gas Reservoir in the Kuqa Depression. *Earth Sci.* **2023**, *48*, 621–639.
44. Zeng, L.B.; Gong, L.; Guan, C.; Zhang, B.J.; Wang, Q.Q.; Zeng, Q.; Lyu, W.Y. Natural fractures and their contribution to tight gas conglomerate reservoirs: A case study in the northwestern Sichuan Basin, China. *J. Pet. Sci. Eng.* **2022**, *210*, 110028. [CrossRef]
45. He, J.H.; Cao, H.X.; Deng, H.C.; Yin, C.H.; Zhu, Y.P.; Li, C.; Li, Y.; Yin, S. Nature fractures in shales of the Lianggaoshan Formation in northern Sichuan Basin: Fracture development characteristics and fracture formation and evolution model. *Earth Sci. Front.* **2024**, *31*, 17–34.
46. Du, X.Y.; Jin, Z.J.; Zeng, L.B.; Liu, G.P.; He, W.J.; Yang, S.; Liang, X.P.; Lu, G.Q. Development Model of Natural Fractures in Continental Shale of the Pingdiquan Formation in the Shuangjingzi Area. *East. Junggar Basin Earth Sci.* **2024**, *49*, 3264–3275.
47. Shang, M.H.; Zhao, X.Y.; Hu, X.Y.; Xiao, K.H.; Liu, G.P. Development Characteristics and Distribution Patterns of Natural Fractures in Continental Reservoirs in the Yuanba Area, Northeast Sichuan. *Fault-Block Oil Gas Field* **2022**, *29*, 8–13.
48. Li, Y.; Hou, G.T.; Hari, K.R.; Neng, Y.; Lei, G.L.; Tang, Y.G.; Zhou, L.; Sun, S.; Zheng, C.F. The model of fracture development in the faulted folds: The role of folding and faulting. *Mar. Pet. Geol.* **2018**, *89*, 243–251. [CrossRef]
49. Watkins, H.; Butler, W.R.; Bond, E.C.; Dave, H. Influence of structural position on fracture networks in the Torridon Group, Achnashellach fold and thrust belt, NW Scotland. *J. Struct. Geol.* **2015**, *74*, 64–80. [CrossRef]
50. Ju, W.; Wang, K.; Hou, G.T.; Sun, W.T.; Yu, X. Prediction of natural fractures in the Lower Jurassic Ahe Formation of the Dibei Gasfield, Kuqa Depression, Tarim Basin, NW China. *Geosci. J.* **2018**, *22*, 241–252. [CrossRef]
51. Xia, L.; Xi, K.L.; Yang, X.Z.; Han, Z.H.; Xu, Z.P.; Zhou, L.; Yu, G.D.; Wang, D.S.; Wang, W.Y. Relationship between Natural Fracture and Structural Style and its Implication for Tight Gas Enrichment: A Case Study of Deep Ahe Formation in the Dibei–Tuzi Area, Kuqa Depression. Acta Geol. *Sin. Engl. Ed.* **2024**, *98*, 1086–1110. [CrossRef]
52. Wu, G.H.; Gao, L.H.; Zhang, Y.T.; Ning, C.Z.; Xie, E. Fracture attributes in reservoir-scale carbonate fault damage zones and implications for damage zone width and growth in the deep subsurface. *J. Struct. Geol.* **2018**, *118*, 181–193. [CrossRef]
53. Maerten, L.; Maerten, F.; Lejri, M. Along fault friction and fluid pressure effects on the spatial distribution of fault-related fractures. *J. Struct. Geol.* **2018**, *108*, 198–212. [CrossRef]
54. Luo, H.Y.; Chen, J.; Zhang, X.Q.; Meng, X.X.; Zhao, F.Q.; Wu, S.J.; Guo, X. Sedimentary Characteristics of Fluvial—Dominated Shallow—Water Delta Fronts and Their Control on Lithologic Reservoirs: A Case Study of the Baxigai Formation in the Southern Slope of the Kuqa Depression. *Lithol. Reserv.* **2021**, *33*, 70–80.
55. Wei, G.Q.; Zhang, R.H.; Zhi, F.Q.; Wang, K.; Yu, C.F.; Dong, C.Y. Formation Conditions and Exploration Directions of Tectonic—Lithostratigraphic Hydrocarbon Reservoirs in the Mesozoic of the Eastern Kuqa Depression. *Acta Pet. Sin.* **2021**, *42*, 1113–1125.
56. Feng, J.R.; Gao, Z.Y.; Cui, J.G.; Zhou, C.M. Reservoir Porosity Evolution Characteristics and Evaluation of the Jurassic Deep Reservoir from Dibei in Kuqa Depression: Insight from Diagenesis Modeling Experiments Under the Influence of Burial Mode. *Adv. Earth Sci.* **2018**, *33*, 305–320.
57. Shi, H.; Luo, X.R.; Lei, G.L.; Wei, H.X.; Zhang, L.Q.; Zhang, L.K.; Lei, Y.H. Effects of early oil emplacement on reservoir quality and gas migration in the Lower Jurassic tight sand reservoirs of Dibei gas field, Kuqa Depression, western China. *J. Nat. Gas Sci. Eng.* **2018**, *50*, 250–258. [CrossRef]
58. Peng, J.; Han, H.D.; Xia, Q.S.; Li, B. Fractal characteristic of microscopic pore structure of tight sandstone reservoirs in Kalpintag Formation in Shuntuoguole area, Tarim Basin. *Pet. Res.* **2020**, *5*, 1–17. [CrossRef]
59. Yuan, W.F. Water-sensitive characterization and its controlling factors in clastic reservoir: A case study of Jurassic Ahe Formation in Northern tectonic zone of Kuqa depression. *Pet. Res.* **2020**, *5*, 77–82. [CrossRef]

60. Nian, T.; Wang, G.W.; Xiao, C.W.; Zhou, L.; Deng, L.; Li, R.J. The in situ stress determination from borehole image logs in the Kuqa Depression. *J. Nat. Gas Sci. Eng.* **2016**, *34*, 1077–1084. [CrossRef]
61. Chen, Z.Q.; Zhou, Z.H.; He, C.; Jiang, C.W.; Wang, B.; Li, T.S. Influence of faults on the geo-stress field distribution and damage evolution mechanism of fracture zones. *Bull. Eng. Geol. Environ.* **2023**, *82*, 173. [CrossRef]
62. Yong, R.; Wu, J.F.; Huang, H.Y.; Xu, E.S.; Xu, B. Complex in situ stress states in a deep shale gas reservoir in the southern Sichuan Basin, China: From field stress measurements to in situ stress modeling. *Mar. Pet. Geol.* **2022**, *141*, 105702. [CrossRef]
63. Wang, Q.; Guo, Z.; Tang, H.; Cheng, G.; Liu, Z.; Zhou, K. Natural Fractures in Tight Sandstone Gas Condensate Reservoirs and Their Influence on Production in the Dina 2 Gas Field in the Kuqa Depression, Tarim Basin, China. *Energies* **2024**, *17*, 4488. [CrossRef]
64. Zhao, X.; Wang, G.; Li, D.; Wang, S.; Sun, Q.; Lai, J.; Han, Z.; Li, Y.; Shen, Y.; Wu, K. Characteristics and Controlling Factors of Natural Fractures in Lacustrine Mixed Shale Oil Reservoirs: The Upper Member of the Lower Ganchaigou Formation in the Ganchaigou Area, Qaidam Basin, Western China. *Energies* **2024**, *17*, 5996. [CrossRef]
65. Suo, Y.; Su, X.H.; He, W.Y.; Fu, X.F.; Ai, C.; Xie, K. Intelligent Prediction of Shale Hydraulic Fracturing Network Evaluation Based on Artificial Intelligence Model. *Sci. Technol. Eng.* **2024**, *2*.

Disclaimer/Publisher's Note: The statements, opinions and data contained in all publications are solely those of the individual author(s) and contributor(s) and not of MDPI and/or the editor(s). MDPI and/or the editor(s) disclaim responsibility for any injury to people or property resulting from any ideas, methods, instructions or products referred to in the content.